

R-06-87

**Earthquake induced rock shear
through a deposition hole when
creep is considered – first model
Effect on the canister and the buffer**

Jan Hernelind, 5T Engineering AB

August 2006

Svensk Kärnbränslehantering AB

Swedish Nuclear Fuel
and Waste Management Co
Box 5864

SE-102 40 Stockholm Sweden

Tel 08-459 84 00
+46 8 459 84 00

Fax 08-661 57 19
+46 8 661 57 19



**Earthquake induced rock shear
through a deposition hole when
creep is considered – first model
Effect on the canister and the buffer**

Jan Hernelind, 5T Engineering AB

August 2006

Keywords: Canister, Copper, Cast iron insert, Bentonite, Buffer, Earthquake, Rock, Shear, Creep, Modeling, Calculation.

This report concerns a study which was conducted for SKB. The conclusions and viewpoints presented in the report are those of the author and do not necessarily coincide with those of the client.

A pdf version of this document can be downloaded from www.skb.se

Abstract

March, 2003, a study regarding “Earthquake induced rock shear through a deposition hole” /4-2/ were performed. Existing fractures crossing a deposition hole may be activated and sheared by an earthquake. The effect of such a rock shear has been investigated in a project that includes both laboratory tests and finite element calculations.

The buffer material in a deposition hole acts as a cushion between the canister and the rock, which reduces the effect of a rock shear substantially. Lower density of the buffer yields softer material and reduced effect on the canister. However, at the high density that is suggested for a repository the stiffness of the buffer is rather high. The stiffness is also a function of the rate of shear, which means that there may be a substantial damage on the canister at very high shear rates.

The rock shear has been modeled with finite element calculations with the code ABAQUS. A three-dimensional finite element mesh of the buffer and the canister has been created and simulation of a rock shear has been performed.

The rock shear has been assumed to take place perpendicular to the canister at the quarter point. The shear calculations have been driven to a total shear of 20 cm.

This report summarizes the effect of considering creep in the canister for one of the previous cases (bwr5b3_case2). Two different creep models have been used – the first one has been suggested by Kjell Pettersson /5-1/ and the second one has been suggested by Rolf Sandström /5-2/. Both have been implemented in the FE-code ABAQUS as a user supplied subroutine CREEP. This report summarizes results obtained by using the first model suggested by Kjell Pettersson. As can be seen from the obtained results using the first creep model (in the following named creep_kp) the effect of creep in copper doesn't affect stresses and strains in the buffer and the steel part very much. However, especially the stresses in the canister are highly affected.

Sammanfattning

Mars, 2003, rapporterades en studie av "Earthquake induced rock shear through a deposition hole" /4-2/. Befintliga sprickor som skär deponeringshål kan aktiveras och skjuvas genom ett jordskalv. Inverkan av en sådan bergskjuvning sammanfattades i ett projekt som omfattade både laboratorieförsök och finita element beräkningar.

Bentonitbufferten i ett deponeringshål fungerar som en kudde mellan kapseln och berget, som avsevärt reducerar inverkan av en bergskjuvning – ju lägre densitet desto mjukare buffert och desto mindre påverkan på kapseln. Vid de höga densiteter som föreslås för bufferten i ett slutförvar är den däremot ganska styv. Styvheten är också en funktion av skjuvhastigheten, vilket medför att kanistern kan skadas avsevärt vid mycket höga skjuvhastigheter.

Bergskjuvningen har modellerats och beräknats med finita-element-koden ABAQUS. Ett tre-dimensionellt elementnät som modellerar bufferten och kapseln har skapats samt simulering av bergskjuvningar har utförts.

I den här rapporten studeras effekten av krypning i kapseln för ett av det tidigare fallen (bwr5b3_case2). Två olika krypmodeller har implementerats i ABAQUS – den första baserad på teori föreslagen av Kjell Pettersson /5-1/ och den andra på teori föreslagen av Rolf Sandström /5-2/. Rapporten redovisar resultat då den första modellen, föreslagen av Kjell Pettersson används. Som framgår av de erhållna resultaten när den första modellen används (i det följande benämnd creep_kp) blir effekten av kryp marginell för buffert och ståldelen. Däremot fås en påtaglig inverkan beträffande spänningsnivån i kapseln.

Contents

| | | |
|-------------------|---|----|
| 1 | Introduction | 7 |
| 2 | Earlier investigations | 9 |
| 2.1 | Effect on the canister and the buffer | 9 |
| 3 | Basic bentonite shear properties | 11 |
| 3.1 | General | 11 |
| 4 | FEM model | 13 |
| 4.1 | General | 13 |
| 4.2 | Finite element mesh | 13 |
| 4.3 | Material models | 13 |
| 4.4 | Bentonite buffer | 15 |
| 4.5 | Cast iron and copper | 16 |
| 4.6 | Basic calculations | 17 |
| 5 | Results from calculation 5b3_case2 (contact elements – no creep effects) | 19 |
| 5.1 | Deformed structure | 19 |
| 5.2 | Stresses in the cast iron insert | 19 |
| 5.3 | Stresses in the copper canister | 19 |
| 5.4 | Stresses in the bentonite buffer | 19 |
| 6 | Results from calculation 5b3_case2_creep (contact elements – creep effects (creep_kp)) | 21 |
| 6.1 | Deformed structure | 21 |
| 6.2 | Stresses in the cast iron insert | 21 |
| 6.3 | Stresses in the copper canister | 21 |
| 6.4 | Stresses in the bentonite buffer | 22 |
| 7 | Comparison and evaluation of the results | 23 |
| 8 | Conclusions | 25 |
| | References | 27 |
| Appendix 1 | Calculation 5b3_case2 | 29 |
| Appendix 2 | Calculation 5b3_case2 using creep_kp | 35 |
| Appendix 3 | User subroutine used for creep analysis (creep_kp) | 57 |

1 Introduction

One important function of the buffer material in a deposition hole in a repository for nuclear waste disposal is to reduce the damage of rock movements on the canister. The worst case of rock movements is probably a very fast shear that takes place along a fracture and occurs as a result of an earthquake.

The consequences of such rock shear has been investigated earlier, both by laboratory tests /1-1/, laboratory simulations in the scale 1:10 /1-2/ and finite element modeling /1-3/ and /1-4/.

- In order to update the results a new investigation has been performed where a creep model has been added to the material definition of the canister.

2 Earlier investigations

The main investigation concerning rock shear through a deposition hole has been earthquake induced rock shear through a deposition hole.

2.1 Effect on the canister and the buffer

The functions and scenarios were simulated by the finite element code ABAQUS. The bentonite was modeled with the stress theory Porous Elasticity and Drucker Prager Plasticity according to a model derived from laboratory investigations.

According to this investigation a rock displacement of 20 cm across the deposition hole will cause some plastic strain in the copper but the plastic strain will be small with a maximum of 4% which was achieved at a bentonite density of 2,000 kg/m³, which is higher than intended for actual use in repositories.

3 Basic bentonite shear properties

3.1 General

The most important buffer property for modeling the effect of a rock shear is the shear strength of the bentonite. The shear strength and the stress-strain properties of compacted bentonite after complete water saturation have been investigated in a number of different tests. The shear strength is a function of mainly the following factors:

- The swelling pressure, which is a function of the density of the bentonite.
- The rate of shear.

The relation between the density and the swelling pressure is well known from earlier investigations. The influence of shear rate on the shear strength has also been investigated earlier and is reported by Børgesson et al. /4-2/.

4 FEM model

4.1 General

The finite element code ABAQUS was used for the calculations. ABAQUS contains a capability of modeling a large range of processes in many different materials as well as complicated three-dimensional geometry. The code includes special material models for rock and soil and ability to model geological formations with infinite boundaries and in situ stresses by e.g. the own weight of the medium. Detailed information of the available models, application of the code and the theoretical background is given in the ABAQUS manuals /4-1/.

4.2 Finite element mesh

The finite element mesh consists of about 500 solid 3D elements. Figure 4-1 shows the entire model of the deposition hole and the three different parts (bentonite buffer, copper canister and cast iron insert). The rock is not modeled but assumed to be completely stiff. The model is symmetric along the axial plane that cuts the deposition hole into two halves. The insert is of the BWR type with 12 channels for fuel assemblies. The shear takes place in a plane perpendicular to the axis of the hole either in the centre or at the $\frac{1}{4}$ point. The dimensions are the following:

- Deposition hole: diameter 1.75 m and length 6.835 m.
- Copper canister: outer diameter 1.05 m and outer length 4.835 m.
- Copper wall thickness: 0.05 m.
- Cast iron insert: diameter 0.949 m and length 4.733 m.
- Wall thickness between fuel assemblies: 0.05 m.

The 0.5 mm slot between the copper canister and the cast iron insert is thus modeled.

4.3 Material models

Three materials have been modeled. The copper canister and the cast iron insert have properties mainly taken from /1-5/. The properties of the bentonite buffer are taken from /4-2/. The shear strength varies with density and rate of shear but only the reference case (density at saturation 2,000 kg/m³ and shear rate 1 m/s) is modeled.



Figure 4-1. Element mesh (from top to bottom) of the entire model, the bentonite buffer, the copper canister and the cast iron insert. The location of the shear planes are marked in the bentonite.

4.4 Bentonite buffer

The bentonite buffer is modeled using only total stresses that don't include the pore water pressure, the reason being the very fast compression and shear. The stress-strain relation is in ABAQUS described with von Mises stress σ_j that describes the “shear stress” or deviatoric stress in three dimensions according to Equation 1.

$$\sigma_j = (((\sigma_1 - \sigma_3)^2 + (\sigma_1 - \sigma_2)^2 + (\sigma_2 - \sigma_3)^2) / 2)^{1/2} \quad (1)$$

where

σ_1 , σ_2 and σ_3 are the major principal stresses.

The model includes an elastic part and a plastic part. Table 4-1 shows the elastic and plastic data.

The relation between Mises stress and engineering strain for bentonite is shown in Figure 4-2.

Table 4-1. Elastic-plastic material data for the bentonite buffer.

| Case no | Elastic part | | Plastic part: von Mises stress σ_j (MPa) at the following plastic strains (ϵ_p) | | | | | | | |
|---------|--------------|-------|---|----------------------|----------------------|----------------------|----------------------|----------------------|----------------------|--------------------|
| | E (MPa) | ν | $\epsilon_p = 0.0$ | $\epsilon_p = 0.002$ | $\epsilon_p = 0.005$ | $\epsilon_p = 0.009$ | $\epsilon_p = 0.013$ | $\epsilon_p = 0.018$ | $\epsilon_p = 0.023$ | $\epsilon_p = 1.0$ |
| 2 | 363 | 0.49 | 3.63 | 4.85 | 5.57 | 5.95 | 6.19 | 6.3 | 6.22 | 6.22 |

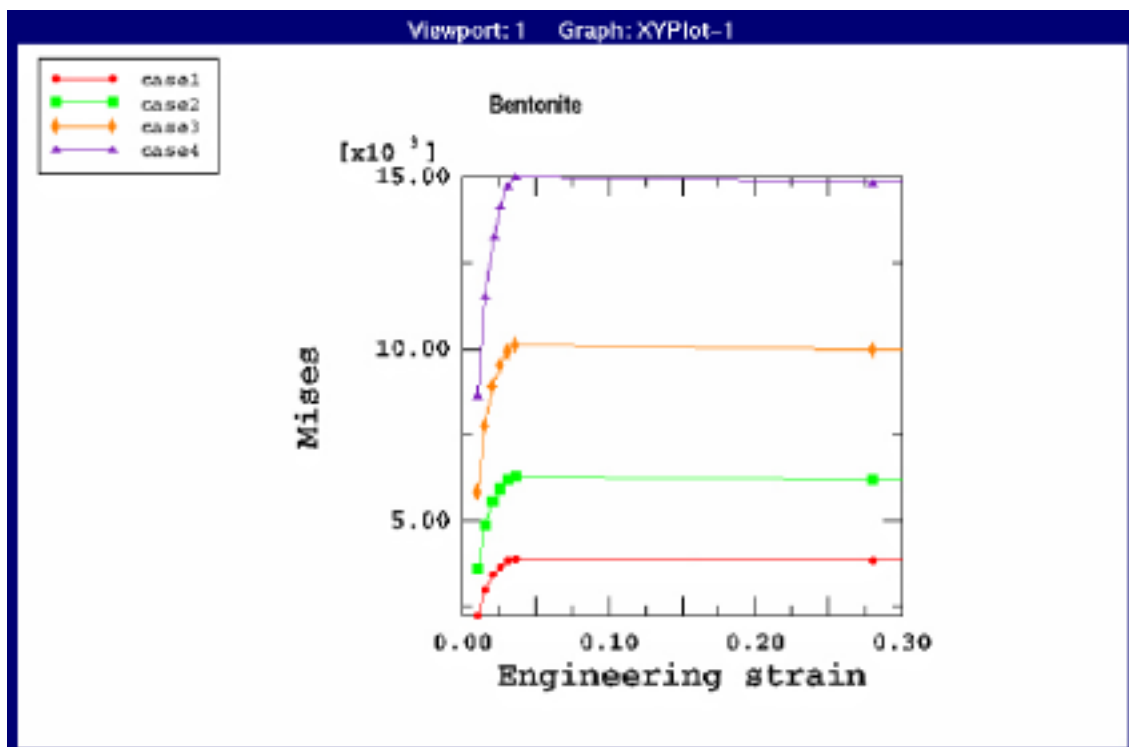


Figure 4-2. Mises stress (kPa) as function of strain for the four cases of bentonite density and the shear rate 1 m/s. Case2 is the reference case.

4.5 Cast iron and copper

The properties of the copper canister and the cast iron insert are also modeled with an elastic plastic model of the Mises stresses. Table 4-2 and Figure 4-3 show the relations.

For copper canister also creep has been included based on one model suggested by Kjell Pettersson /5-1/ and another model suggested by Rolf Sandström /5-2/. The model by Kjell Pettersson used in this study has all material properties built in with, e.g. a yield stress of 20 MPa and strain hardening defined by a strain hardening factor $AM=1.05$ (the coding is shown in Appendix 3 and for details, see the reference /5-1/). The model suggested by Rolf Sandström has also built in materials properties.

Table 4-2. Elastic-plastic material data for the copper and cast iron.

| Material | Elastic part | | Plastic part: von Mises stress σ_j (MPa) at the following plastic strains (ϵ_p) | | | |
|-----------|------------------|------|---|--------------------|--------------------|--------------------|
| | E (MPa) | N | $\epsilon_p = 0$ | $\epsilon_p = 0.2$ | $\epsilon_p = 0.5$ | $\epsilon_p = 1.0$ |
| Copper | $1.2 \cdot 10^5$ | 0.33 | 50 | – | 200 | 200 |
| Cast iron | $1.5 \cdot 10^5$ | 0.32 | 260 | 400 | – | 400 |

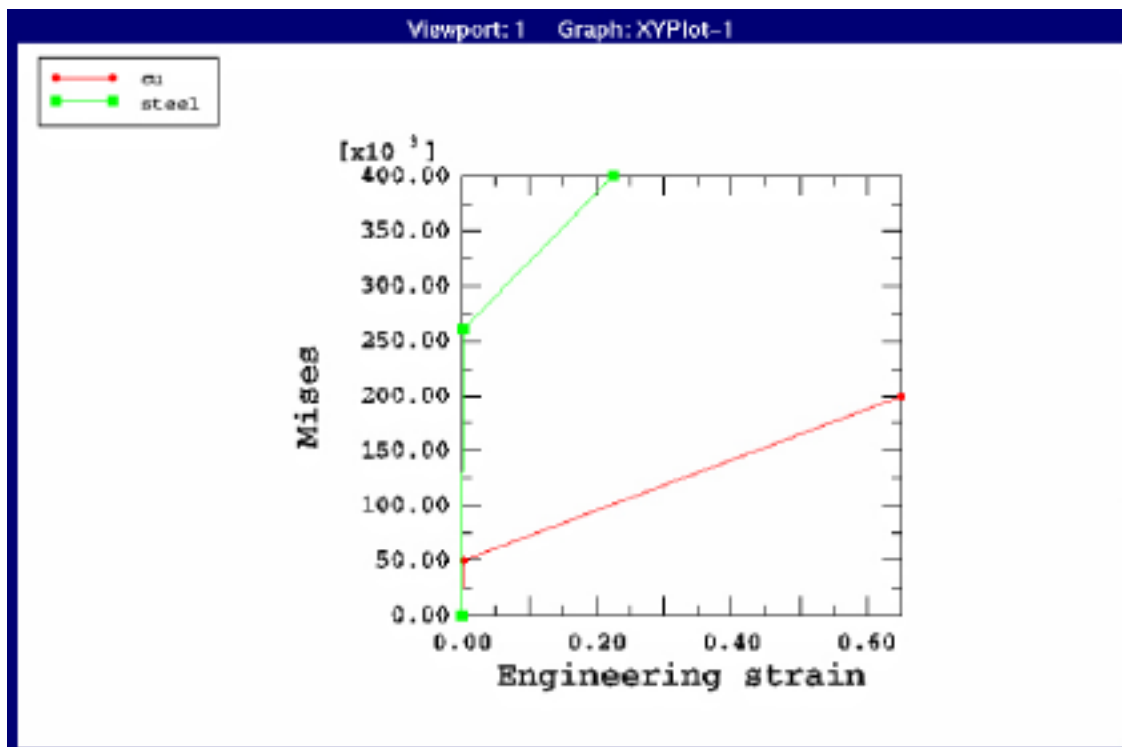


Figure 4-3. Mises stress (kPa) as function of strain for copper and cast iron.

4.6 Basic calculations

The calculations have been done in three steps. At first the swelling pressure has been applied, which mainly has resulted in a deformation of the copper canister due to the closure of the 1 mm gap between the copper and cast iron. Then the shear has started and continued until a total shear displacement of 20 cm. The applied swelling pressure does not influence the shear calculation in any other respect than the initial deformation and induced stresses. Finally the creep effect has been studied for a time period of 100,000 years. Note that the creep effect was taken into account also during the pre-deformation process.

In this calculation the canister has been surrounded by contact elements that cannot withstand any tension. These elements will instead separate in the case of tension stresses. In case of compression the elements have Mohr-Coulomb friction properties with the friction coefficient 0.1 (friction angle 5.7 degrees). Eccentric shear and the density 2,000 kg/m³ were used (*5b3 case2*).

5 Results from calculation 5b3_case2 (contact elements – no creep effects)

This case is used as reference case since it concerns the reference density after full saturation of the buffer (2,000 kg/m³) and the asymmetric shear case, which yields higher stresses in the canister than the symmetric shear at this density.

The results are reported in Appendix 1 as displaced structures, contour plots of stresses and plastic strain after full shearing and as history plots of stresses and plastic strain in the most affected elements. The calculation is identical to one of the calculations in /4-2/.

5.1 Deformed structure

Figure A1-1 shows the deformed structure after complete shearing and also the deformed canister. A rather strong effect on the canister can be seen already in this figure.

Figure A1-2 shows the deformed copper canister and cast iron insert where the deformations are magnified by a factor of 5.

5.2 Stresses in the cast iron insert

Figures A1-3 and A1-4 show the stress and plastic strain (PEEQ) in the cast iron insert on the outside and inside of the cast iron structure. Since the shear plane is located 8 elements (about 0.8 m) from the bottom of the cast iron insert it is obvious that the largest strains are not located at the shear plane but about 1.0 m away towards the centre. The figure reveals that the cast iron insert is deformed substantially and the largest plastic strain is about 4%.

5.3 Stresses in the copper canister

Figure A1-5 shows the plastic strain in the copper canister. The maximum plastic strain is about 4% on the canister envelope surface while it is locally much higher at the lid.

5.4 Stresses in the bentonite buffer

Figure A1-6 shows the plastic strain and the average stress (pressure) in the bentonite buffer. The figures show that a large part of the buffer is plasticized and that the plastic strain locally is several hundred percent. The buffer is also strongly pressurized on the active side of the canister while there is locally very strong tension on the passive side. The bentonite is modeled to be tied to the canister with no limitations in tension stresses, which may yield that kind of unrealistic results.

6 Results from calculation 5b3_case2_creep (contact elements – creep effects (creep_kp))

This case is used as reference case since it concerns the reference density after full saturation of the buffer (2,000 kg/m³) and the asymmetric shear case, which yields higher stresses in the canister than the symmetric shear at this density.

The results are reported in Appendix 2 as displaced structures, contour plots of stresses, plastic strain after full shearing and creep strain after 100,000 years of creep and as history plots of creep strain in the most affected element.

6.1 Deformed structure

Figure A2-1 shows the deformed structure after complete shearing and a part of the structure divided at the shear plane. A rather strong effect on the canister can be seen already in this figure.

Figure A2-2 shows the deformed copper canister with a magnification of the displacements with a factor 5 in order to enhance the effect.

6.2 Stresses in the cast iron insert

Figures A2-11 to A2-14 show the plastic strain in the cast iron insert after respectively 10 and 20 cm shearing followed by creep for 100,000 years. The values are close to the case when creep is neglected (Figure A1-4). Figure A2-15 shows maximum plastic equivalent strain (PEEQ) versus shear displacement and after 20 cm shearing PEEQ is about 3.5%.

6.3 Stresses in the copper canister

Figure A2-17 shows the Mises stress in the copper canister. The maximum Mises stress is about 110 MPa after 20 cm shearing. Figure A2-19 shows the maximum Mises stress after creep for 100,000 years. Maximum value is 51 MPa and thus a substantial reduction of the stress. Figures A2-20 to A2-24 show the corresponding plastic strain – as can be seen the plastic strain is not affected much by creep. Figure A2-22 shows maximum plastic strain versus shear displacement.

Figure A2-26, A2-28 and A2-30 show the creep strain which increases from about 1% after 20 cm shearing to 11.5% after creep for 100,000 years (the maximum value occurs in the lid – the elements are highlighted in Figure A2-31 and the corresponding time history plot of creep strain (CEEQ) is shown in Figure A2-33). In the center part the corresponding maximum creep strain is 0.9%.

The plastic strains, especially close to the lid, will be lower when creep is included since some of the strains actually will be decomposed into creep strain.

6.4 Stresses in the bentonite buffer

Figure A2-4 shows the plastic strain and the average stress (pressure) in the bentonite buffer after 20 cm shearing and Figure A2-6 after creep for 100,000 years. The figures show almost identical results as when creep is neglected (Figure A1-6).

Figure A2-8 shows the average stress (pressure) in the bentonite buffer after 20 cm shearing and Figure A2-10 after creep for 100,000 years. It can be noticed that the values are slightly lower compared to the case when creep is neglected (Figure A1-6).

Note there are discrepancies between what can be seen from the contour plots and what actually exist in the integration points, especially Mises stress and Equivalent plastic strain (PEEQ) will show much higher values in the contour plots due to large gradients inside each element.

7 Comparison and evaluation of the results

A summary of the results is given in Table 7-1 and Table 7-2. The tables show the maximum plastic strain ε_p in the copper tube (Table 7-1 excluding the lid and Table 7-2 when the lid is included), the rock shear displacement δ_p when the plasticization of the cast iron insert starts and the maximum plastic strain ε_p at two different rock shear displacements (10 and 20 cm) with and with out creep considered in the canister.

Table 7-1. Calculated maximum plastic strain ε_p and maximum creep strain ε_c in the copper envelope surface at different rock displacement δ (δ_p = start plasticization). The lid is excluded.

| Shear plane location/ density (kg/m ³) | Copper tube Max ε_c (%) | δ_p (cm) | ε_p (%) at $\delta = 10$ cm | ε_p (%) at $\delta = 20$ cm |
|---|--|--------------------|--|--|
| 2,000 w/o creep | – | 4.5 | 1.4 | 3.3 |
| 2,000 with creep_kp (10 cm shearing) | 0.5 | 4.5 | 0.9 | – |
| 2,000 with creep_kp (20 cm shearing) | 0.9 | 4.5 | 0.9 | 2.4 |

Table 7-2. Calculated maximum plastic strain ε_p and maximum creep strain ε_c in the copper envelope surface (Cu) and cast iron insert (Fe) at different rock displacement δ (δ_p = start plasticization). The lid is included.

| Shear plane location/ density (kg/m ³) | Copper tube Max ε_c (%) | δ_p (cm) | | ε_p (%) at $\delta = 10$ cm | | ε_p (%) at $\delta = 20$ cm | |
|---|--|-----------------|-----|--|-----|--|-----|
| | | Cu | Fe | Cu | Fe | Cu | Fe |
| 2,000 w/o creep | – | 3 | 2.5 | 5.0 | 1.3 | 7.2 | 3.8 |
| 2,000 with creep_kp (10 cm shearing) | 7.6 | 3 | 2.5 | 4.3 | 1.3 | – | – |
| 2,000 with creep_kp (20 cm shearing) | 11.5 | 3 | 2.5 | 4.3 | 1.3 | 6.8 | 3.6 |

8 Conclusions

The effect of an earthquake induced rock shear through a deposition hole when creep is considered in the canister has been studied. The calculations were done with an assumed shear rate of 1.0 m/s at the buffer density 2,000 kg/m³. The creep effect has been analyzed by using a creep theory suggested by Kjell Pettersson /5-1/ .

The *influence of the magnitude of the shear displacement* logically seems to be rather strong when the canister is prevented from tilting with a plastic strain that usually is more than doubled at an increase in shear displacement from 10 cm to 20 cm. However, the effect on the global deformation when creep is taken into consideration is rather minor.

The *copper canister* is strongly plasticized according to these calculations when using creep_kp, especially at the high densities and including creep implies that the peak stress is reduced but the total strain increases due to creep. For this case the maximum creep strain occurs close to the top cover where the maximum creep strain is 11.5%. Close to the center of the copper tube maximum creep strain is about 0.9% and the equivalent plastic strain (PEEQ) is 2.4% when shearing for 20 cm. For the mid part it seems (Table 7-1) as the total strain isn't affected by creep (plastic+creep strain is almost constant).

The plastic strain in the cast iron was, in contrary to the copper, not affected significantly by *introducing creep*.

According to these calculations the creep seems to have minor influence on the results except for the neighborhood of the lid in the copper canister where the creep strains are rather high.

References

- /1-1/ **Börgesson L, Hökmark H, Karnland O, 1988.** Rheological properties of sodium smectite clay. SKB Technical Report 88-30, Svensk Kärnbränslehantering AB.
- /1-2/ **Börgesson L, 1986.** Model shear tests of canisters with smectite clay envelopes in deposition holes. SKB Technical Report 86-26, Svensk Kärnbränslehantering AB.
- /1-3/ **Börgesson L, 1988.** Modelling of buffer material behaviour. Some examples of material models and performance calculations. SKB Technical Report 88-29, Svensk Kärnbränslehantering AB.
- /1-4/ **Börgesson L, 1992.** Interaction between rock, bentonite buffer and canister. FEM calculations of some mechanical effects on the canister in different disposal concepts. SKB Technical Report 92-30, Svensk Kärnbränslehantering AB.
- /1-5/ **Andersson C-G, 2002.** Development of fabrication technology for copper canisters with cast inserts. Status report in August 2001. SKB TR-02-07, Svensk Kärnbränslehantering AB.
- /4-1/ **ABAQUS Manuals.** ABAQUS Inc.
- /4-2/ **Börgesson L, Hernelind J, Johannesson L-E, 2003.** Earthquake induced rock shear through a deposition hole. SKB TR-04-02, Svensk Kärnbränslehantering AB.
- /5-1/ **Pettersson K, 1995.** A Constitutive Model for Plastic deformation and Creep of Copper. Project PM 96-3420-17.
- /5-2/ **Sandström R, Andersson H, 2006.** Representation of creep in Cu-OFP during power-law breakdown. Utkast 06-02-01.

Calculation 5b3_case2

Asymmetric shear at the buffer density 2,000 kg/m³

Creep in canister neglected.

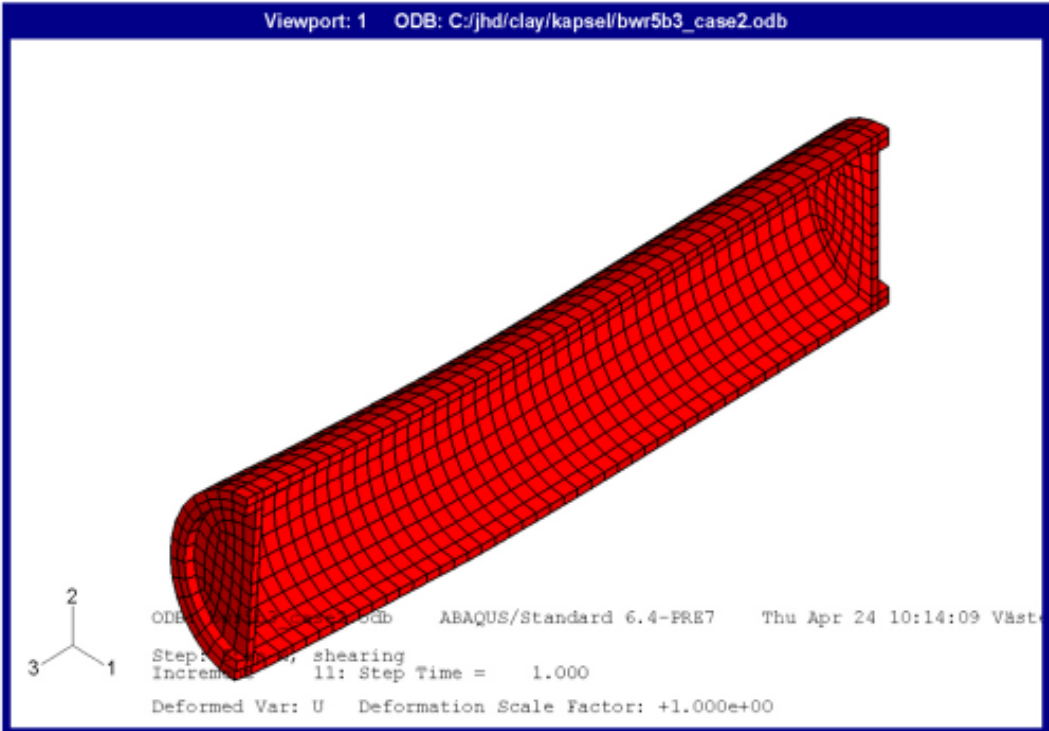
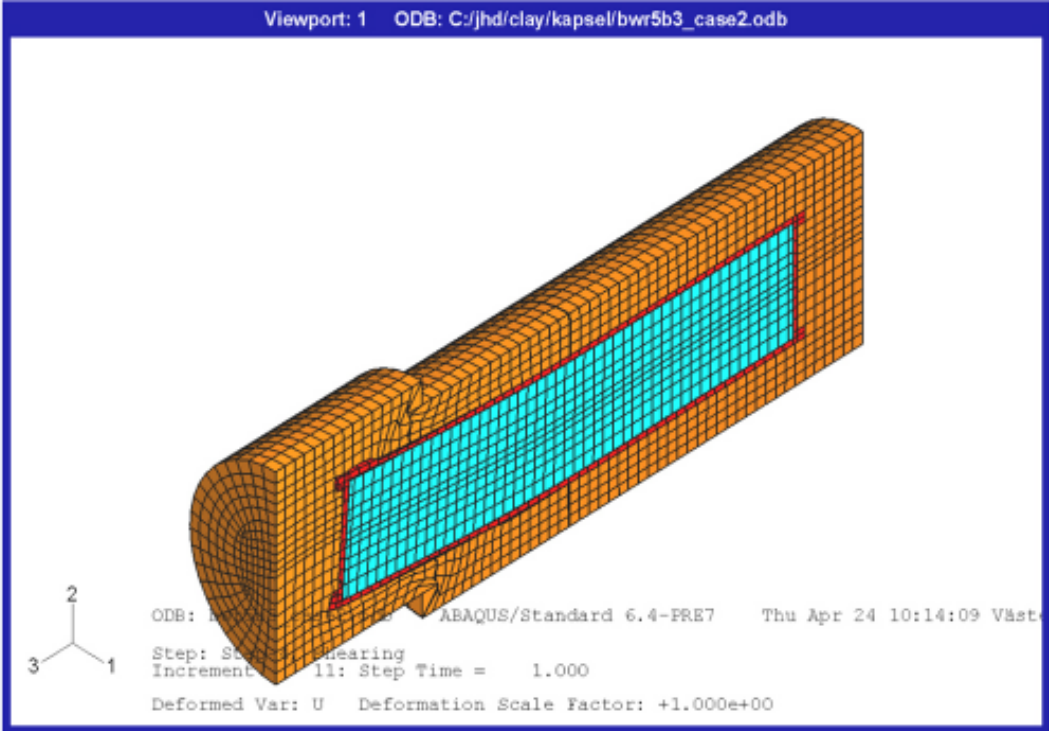


Figure A1-1. Deformed structure after 20 cm rock displacement (upper) and the deformed copper canister (lower).

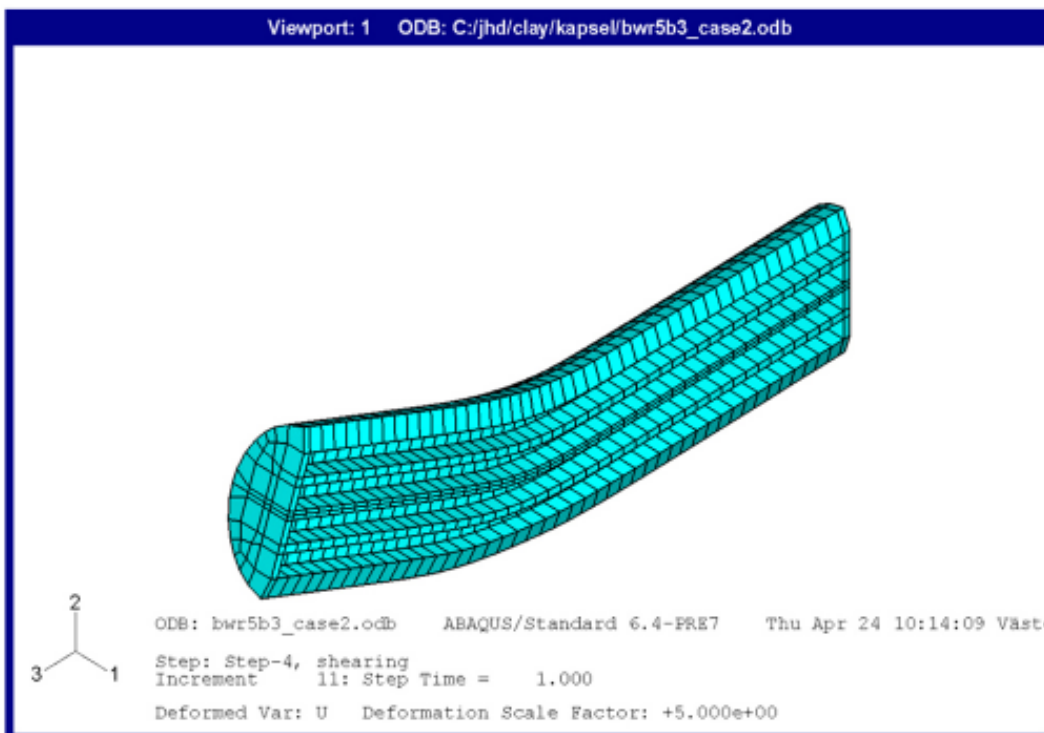
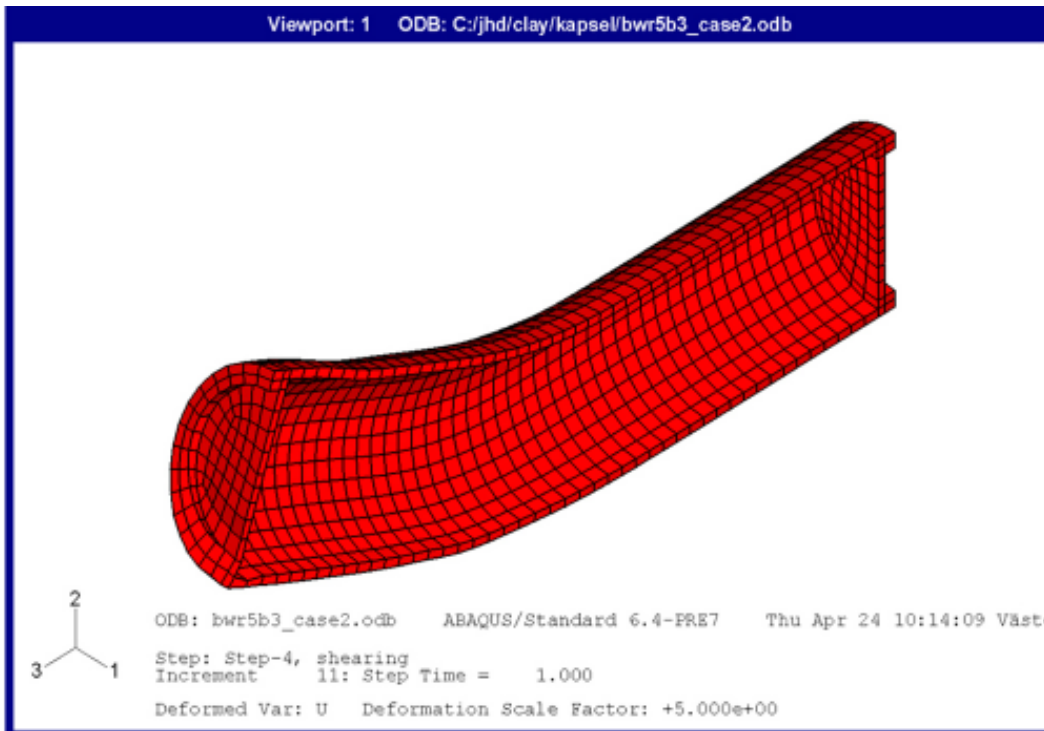


Figure A1-2. Deformed copper canister (upper) and cast iron insert (lower) after 20 cm rock displacement with a deformation magnification factor of 5.

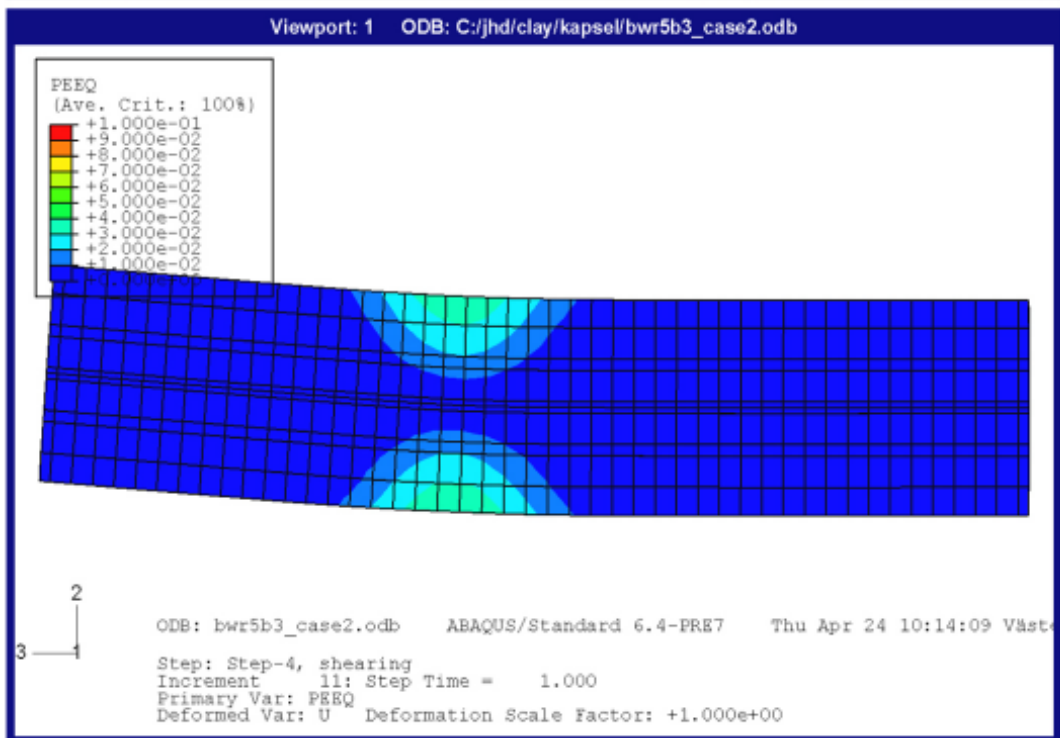
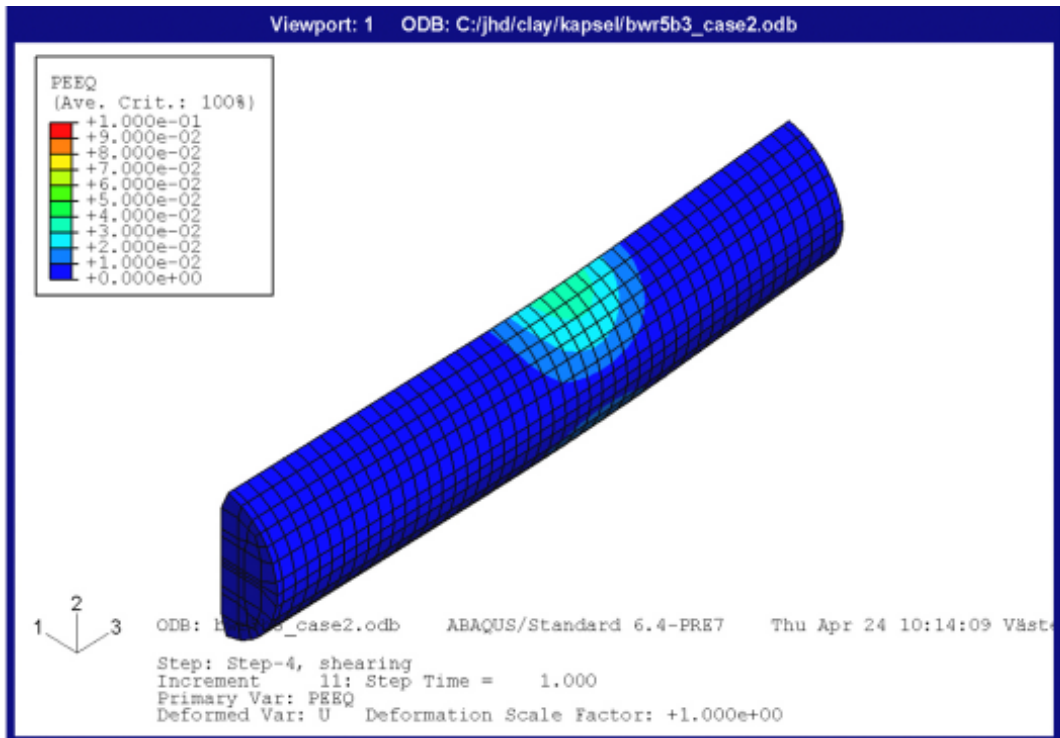


Figure A1-3. Contour plots of the plastic strain in the cast iron insert seen from “behind” (upper) and straight “from the front” (lower) after 20 cm rock displacement. The shear plane is located 8 elements from the left side in the lower figure.

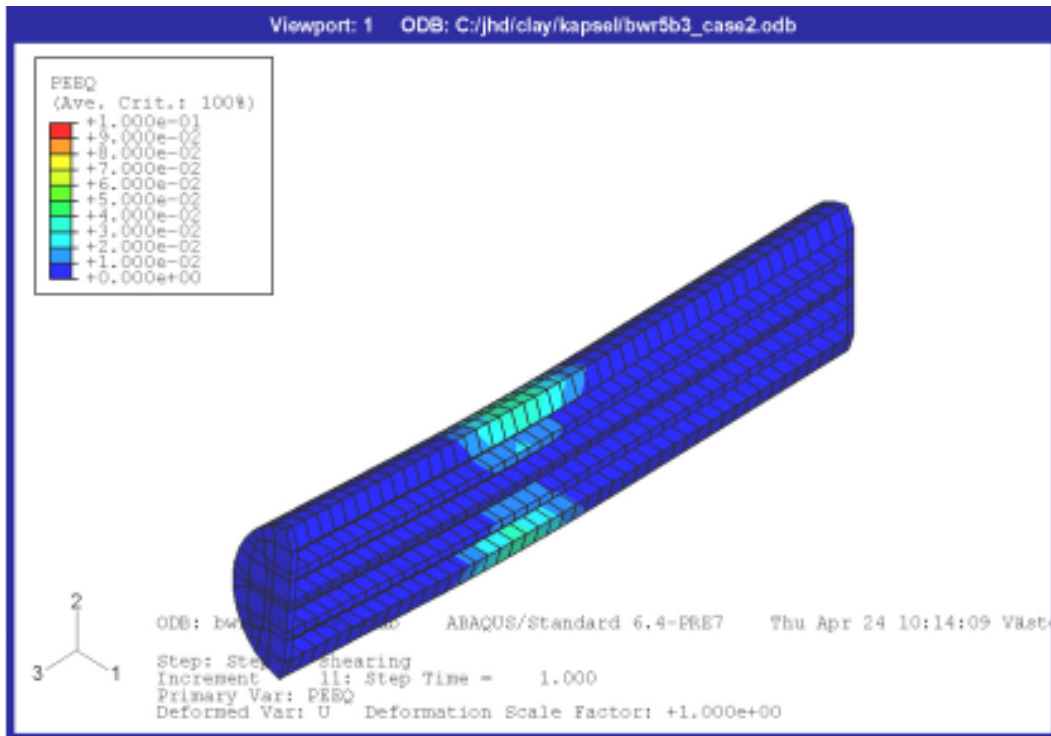


Figure A1-4. Plastic strain in the cast iron insert after 20 cm rock displacement at a section cut parallel to the axis.

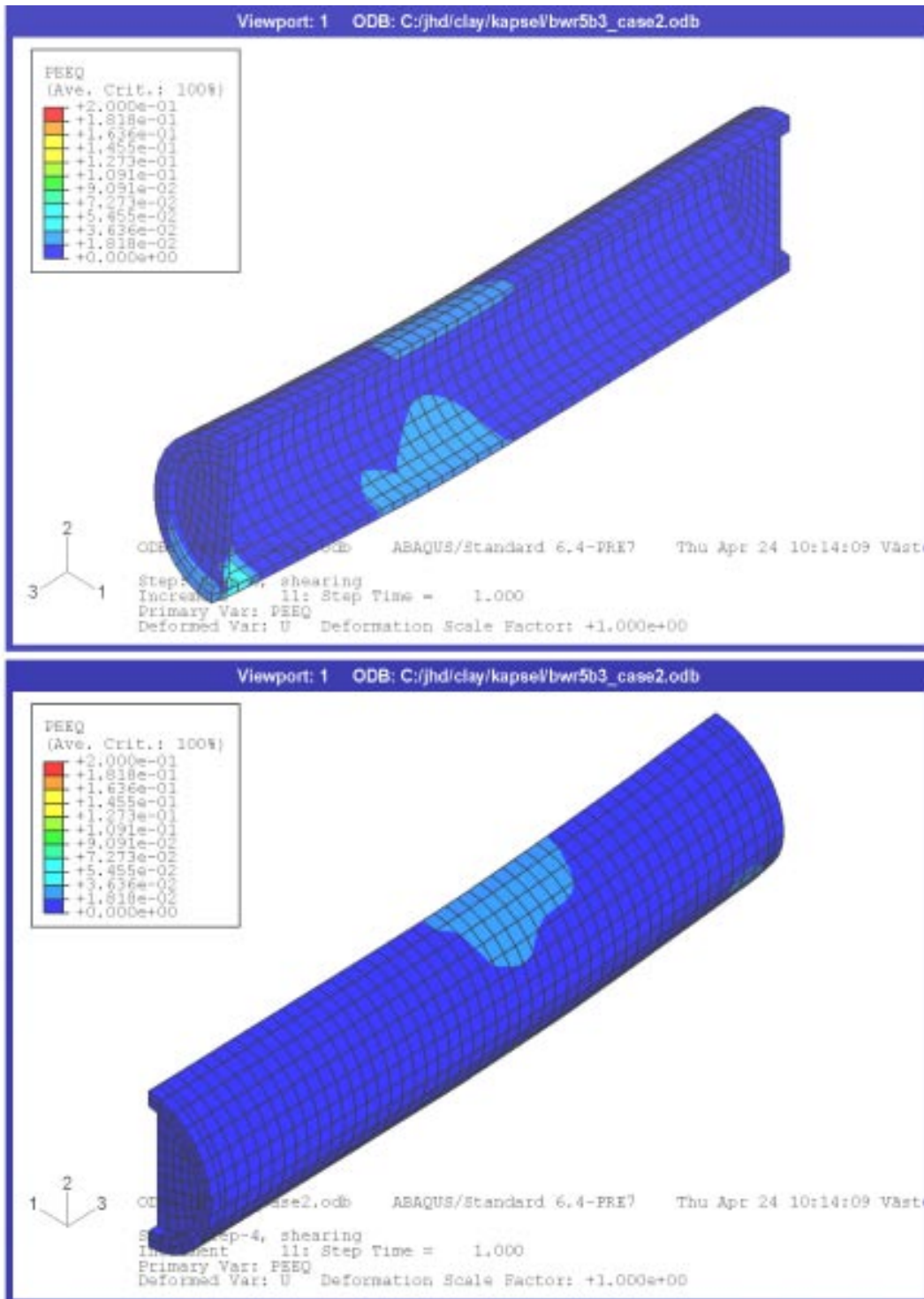


Figure A1-5. Plastic strain in the copper canister after 20 cm rock displacement.

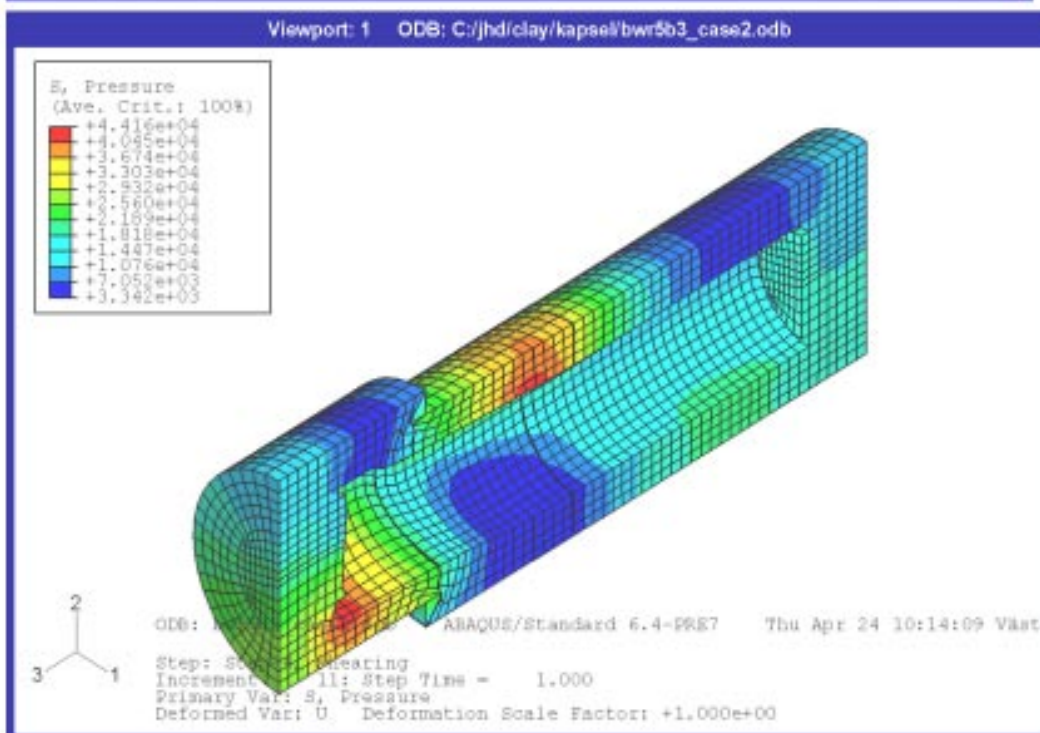
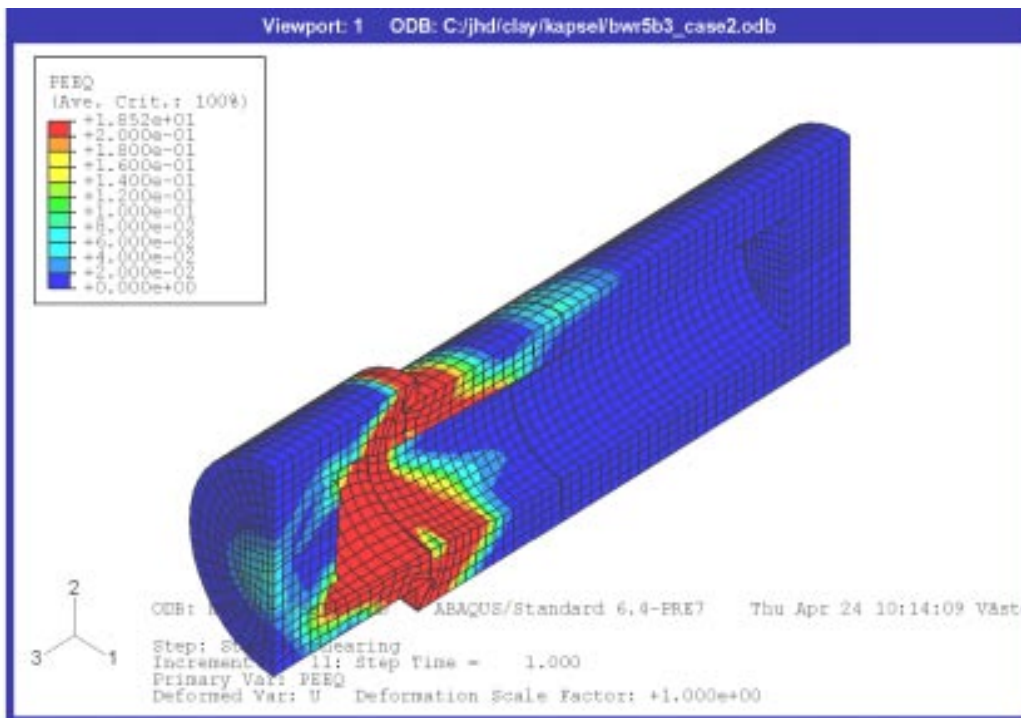


Figure A1-6. Plastic strain (upper) and average stress (kPa pressure) (lower) in the bentonite buffer after 20 cm rock displacement

Calculation 5b3_case2 using creep_kp

Asymmetric shear at the buffer density 2,000 kg/m³

Creep in canister is taken into account. using creep_kp.

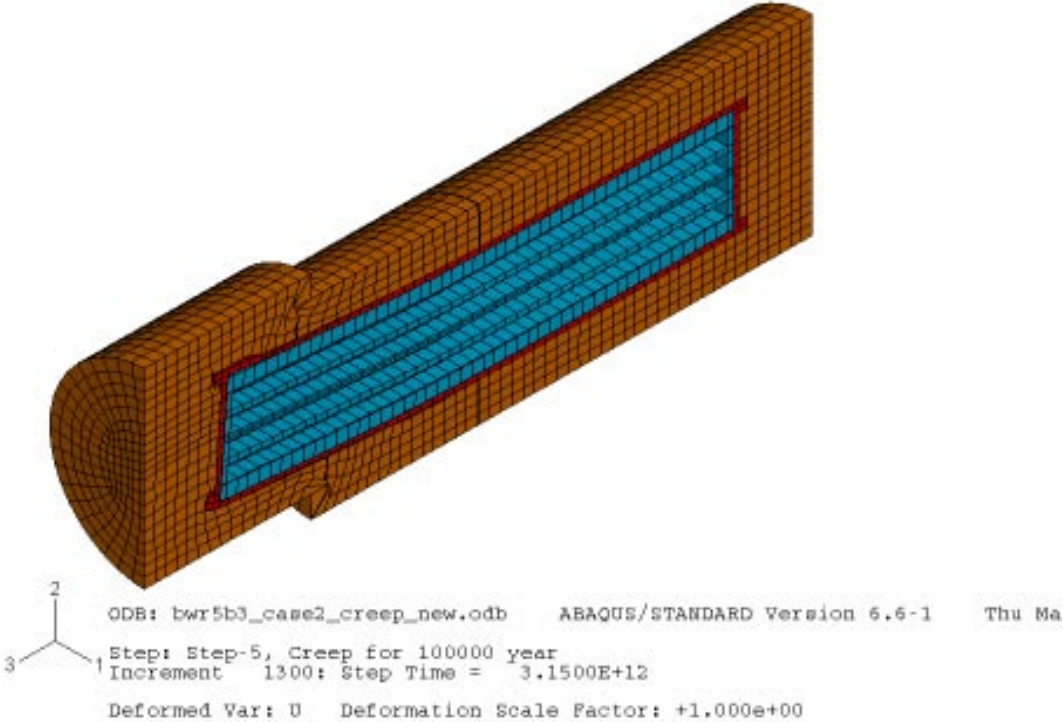


Figure A2-1. bwr5b3_case2 deformed shape after creep for 100,000 years.

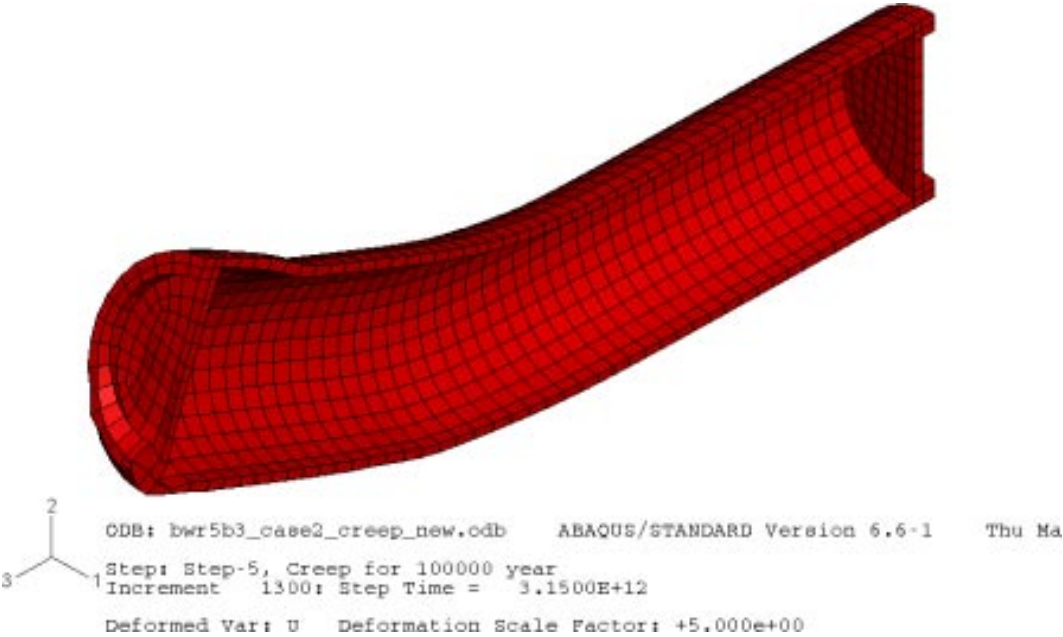


Figure A2-2. bwr5b3_case2 – deformed shape of canister after creep for 100,000 years (magnified by 5).

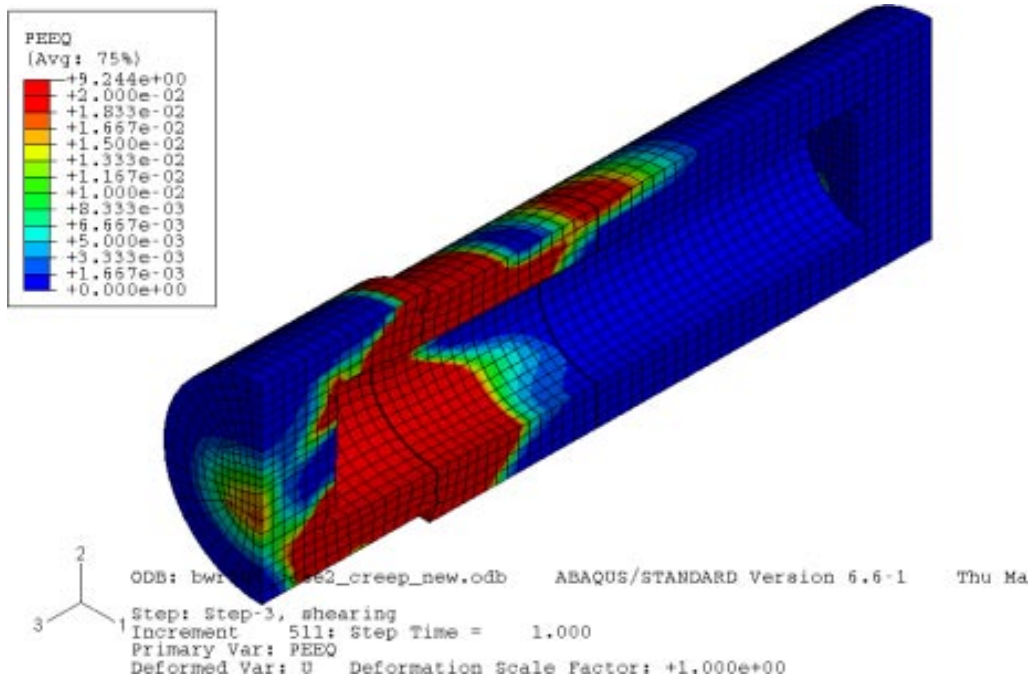


Figure A2-3. bwr5b3_case2 – plastic strain after shearing 10 cm.

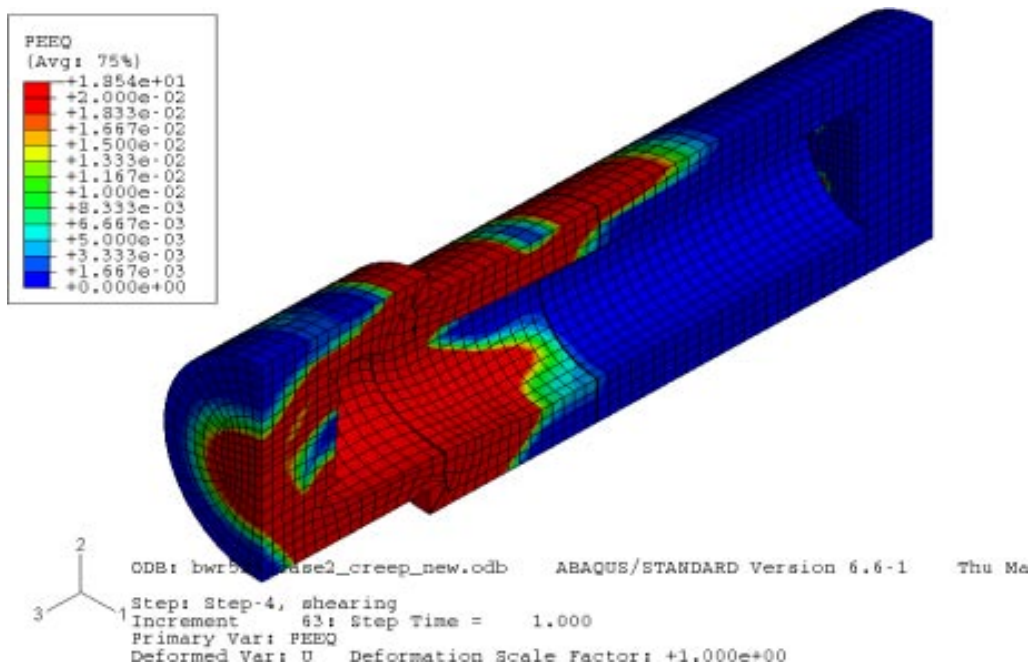


Figure A2-4. bwr5b3_case2 – plastic strain after shearing 20 cm.

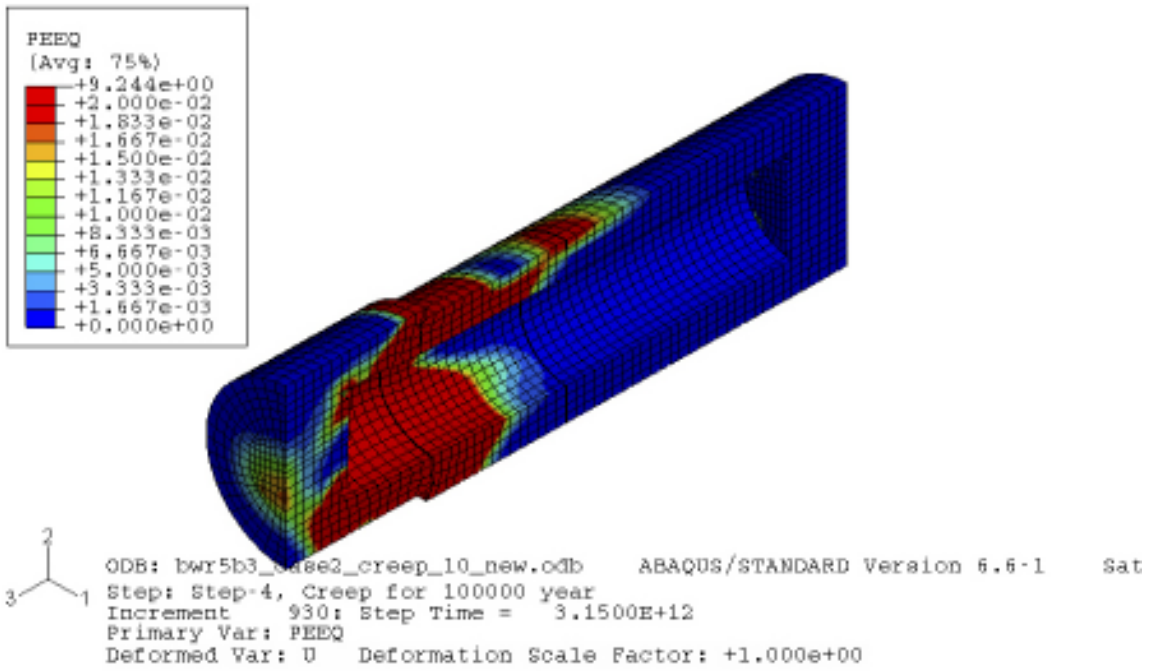


Figure A2-5. bwr5b3_case2 – plastic strain after creep for 100,000 years with 10 cm of shearing.

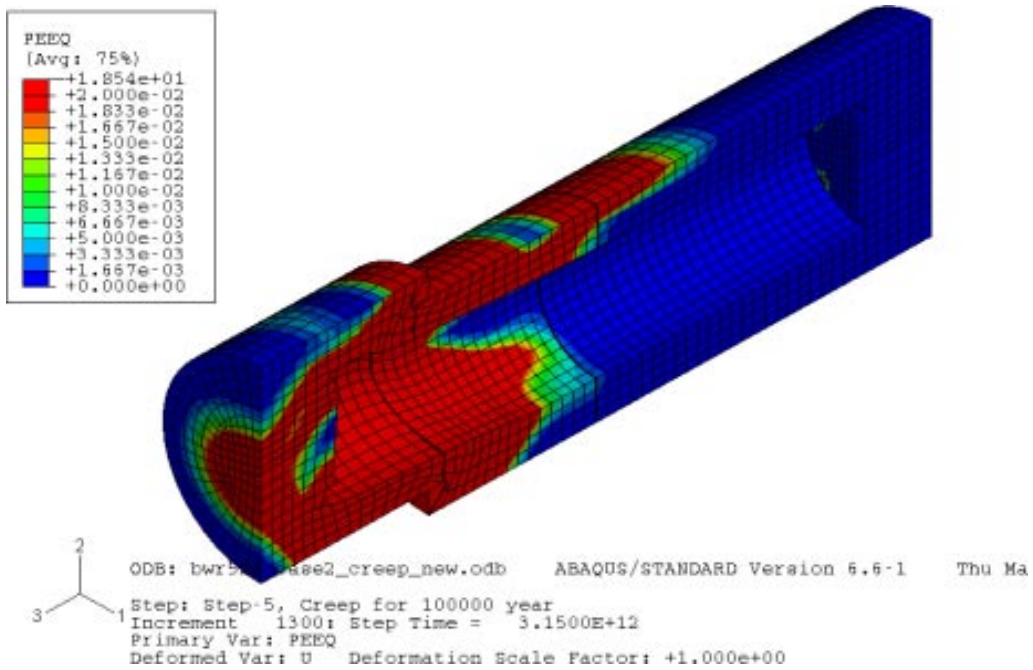


Figure A2-6. bwr5b3_case2 – plastic strain after creep for 100,000 years with 20 cm of shearing.

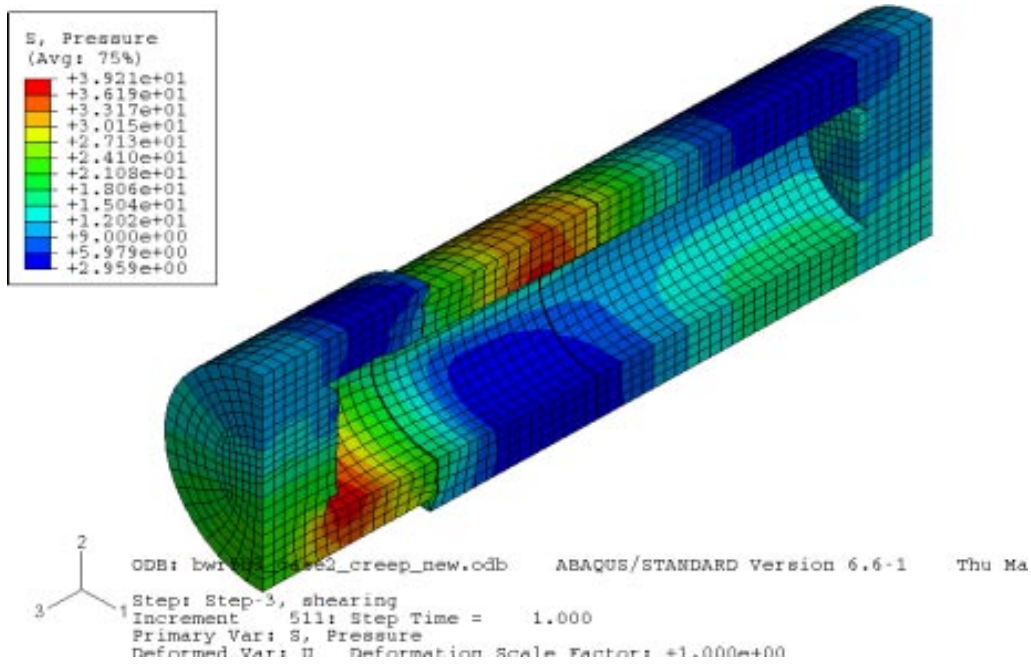


Figure A2-7. bwr5b3_case2 – effective pressure in the bentonite after shearing 10 cm.

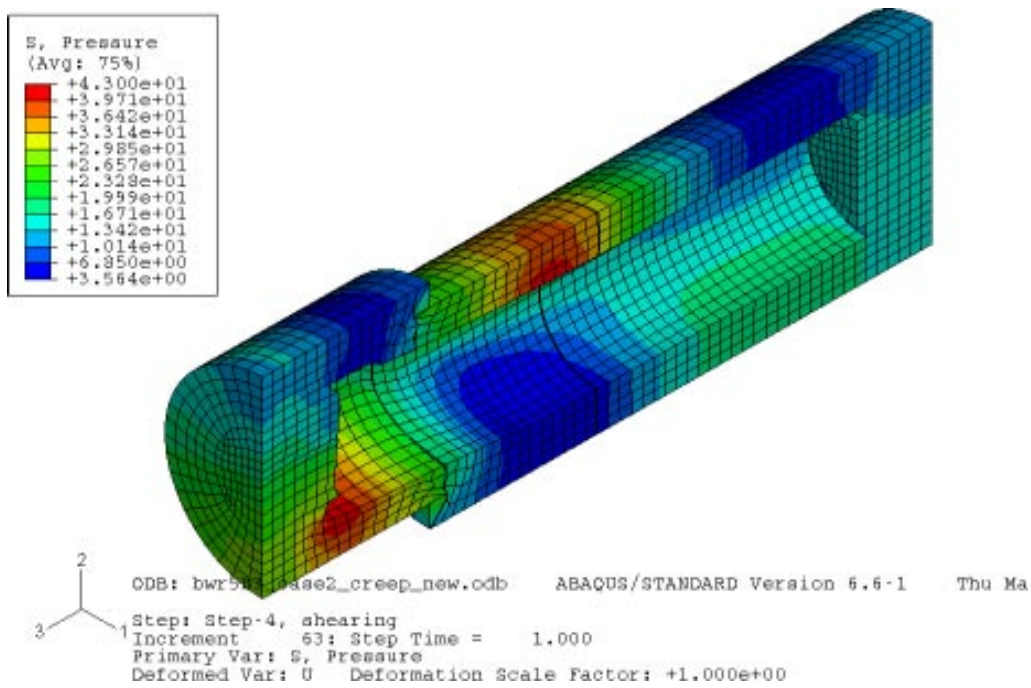


Figure A2-8. bwr5b3_case2 – effective pressure in the bentonite after shearing 20 cm.

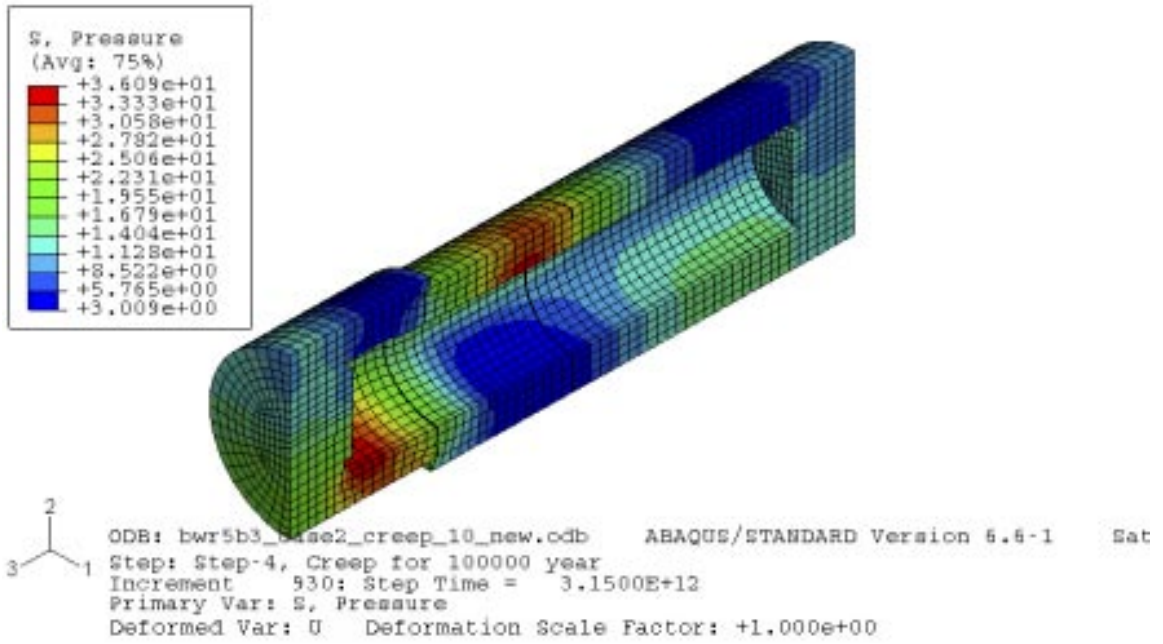


Figure A2-9. bwr5b3_case2 – effective pressure in the bentonite after creep for 100,000 years with 10 cm shearing.

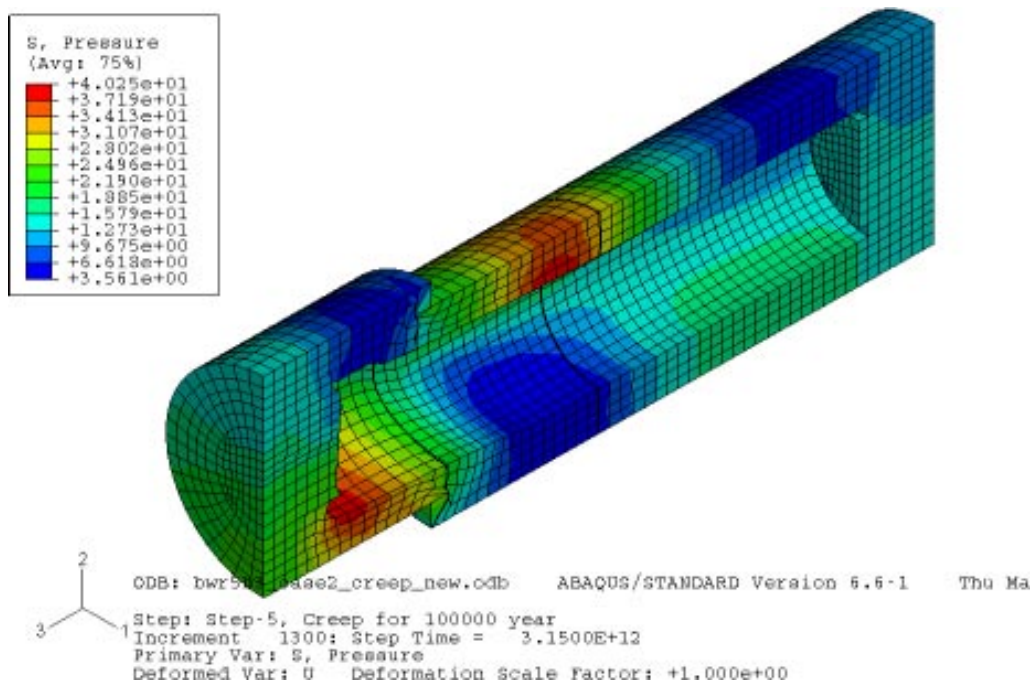


Figure A2-10. bwr5b3_case2 – effective pressure in bentonite after creep for 100,000 years with 20 cm shearing.

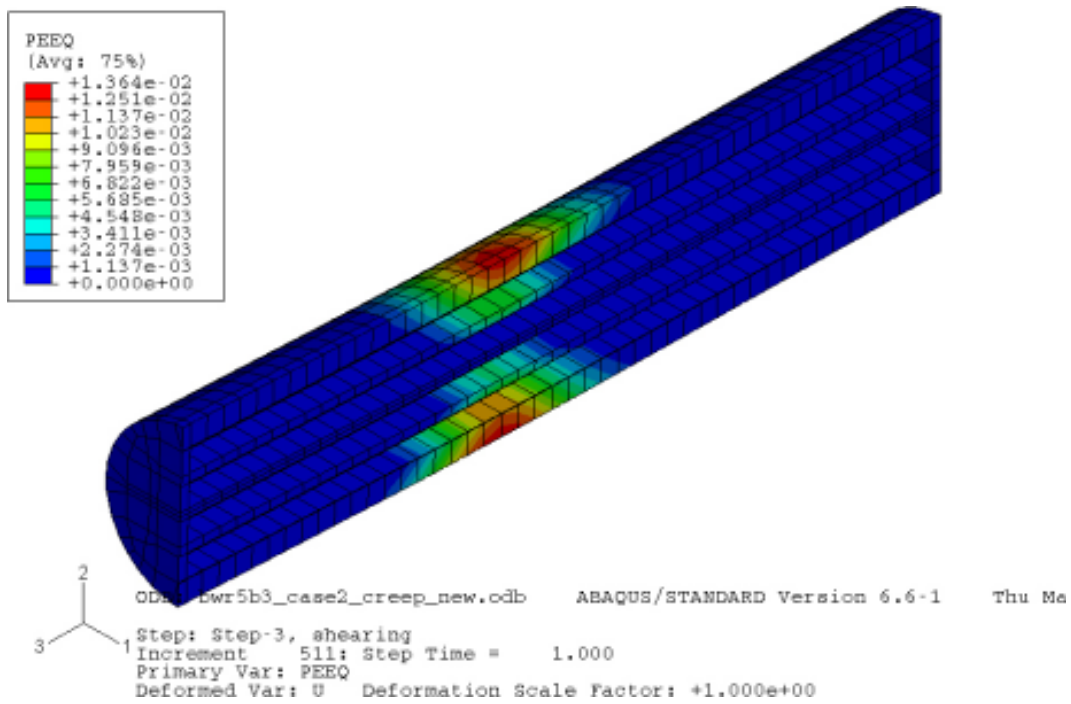


Figure A2-11. bwr5b3_case2 – plastic strain in the steel insert after shearing 10 cm.

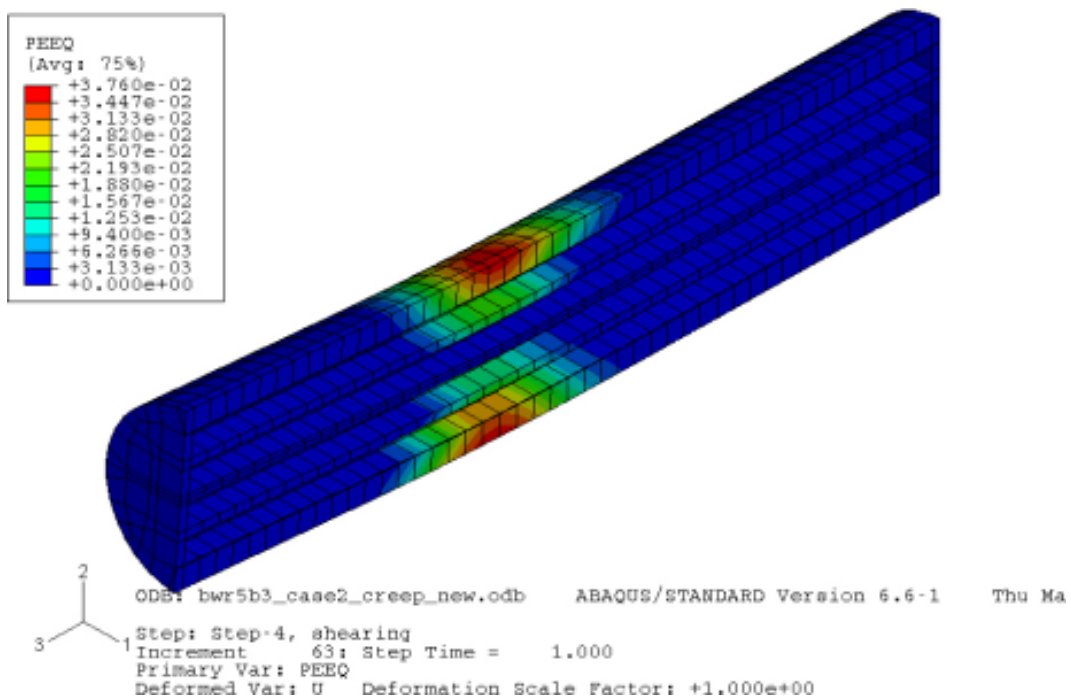


Figure A2-12. bwr5b3_case2 – plastic strain in the steel insert after shearing 20 cm.

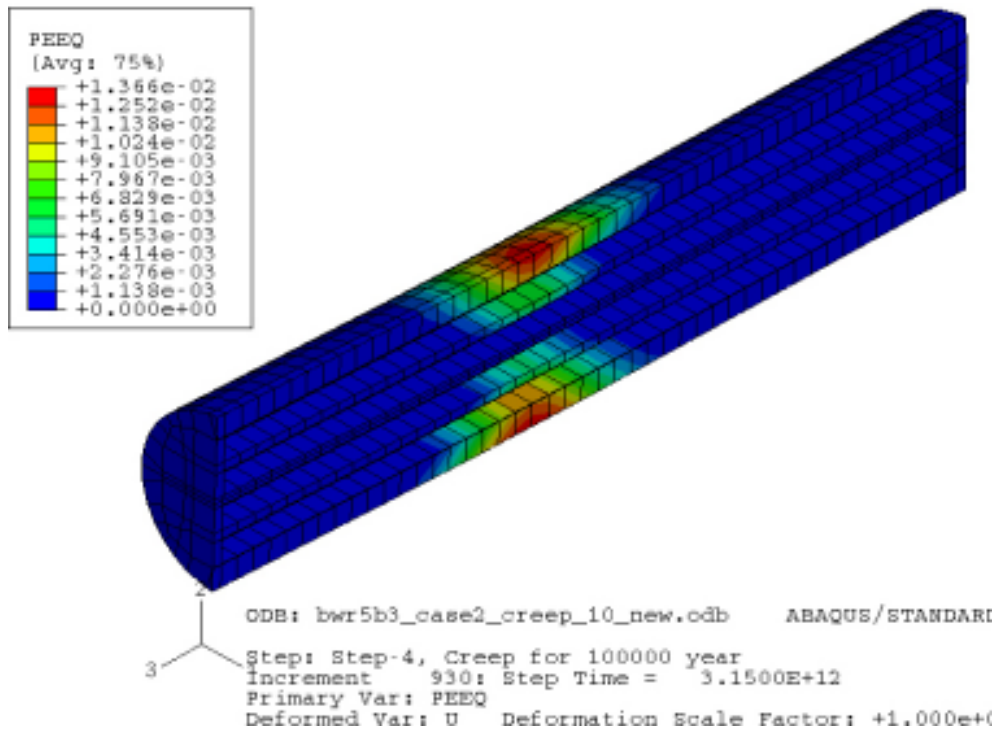


Figure A2-13. bwr5b3_case2 – plastic strain in steel after creep for 100,000 years with 10 cm of shearing.

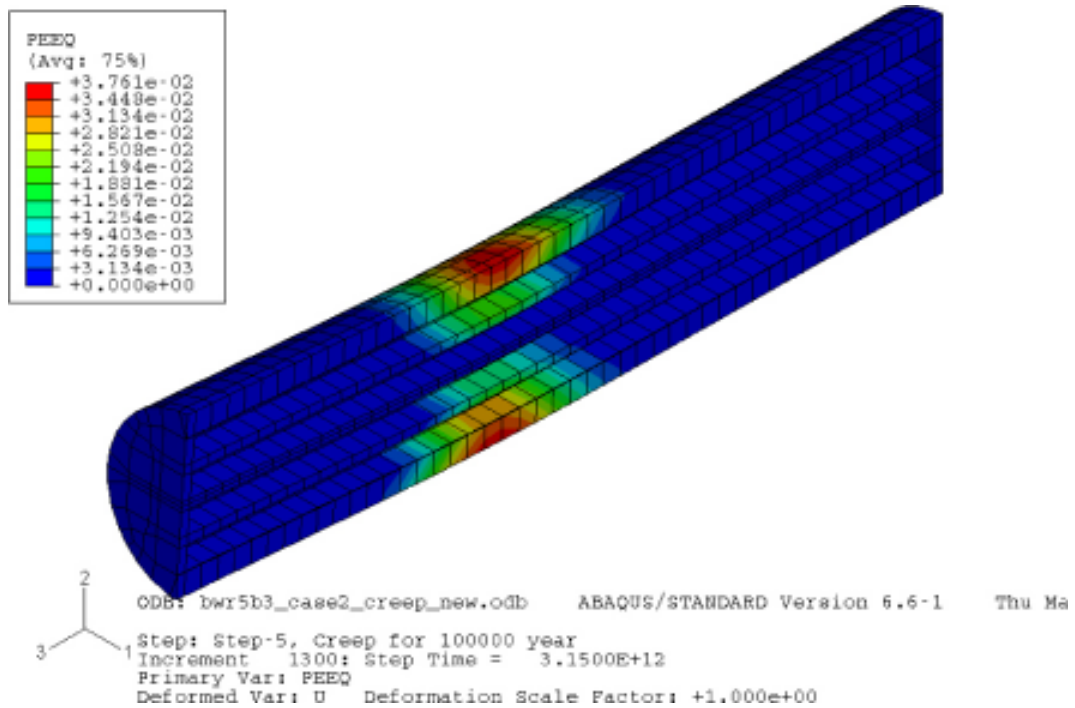


Figure A2-14. bwr5b3_case2 – plastic strain in steel after creep for 100,000 years with 20 cm of shearing.

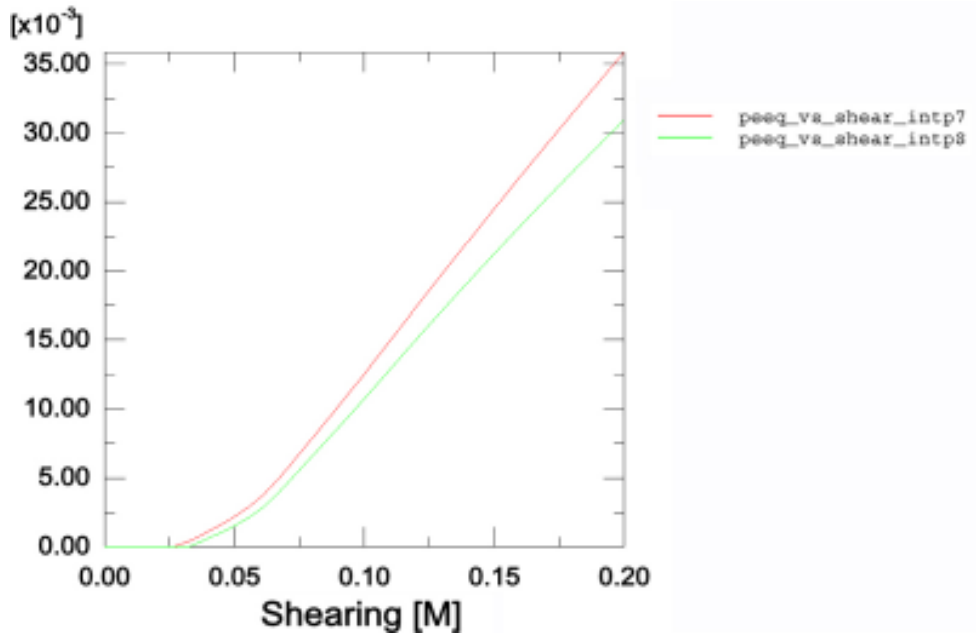


Figure A2-15. bwr5b3_case2 – maximum plastic strain in the steel insert after 20 cm of shearing. Int.point 7 and 8.

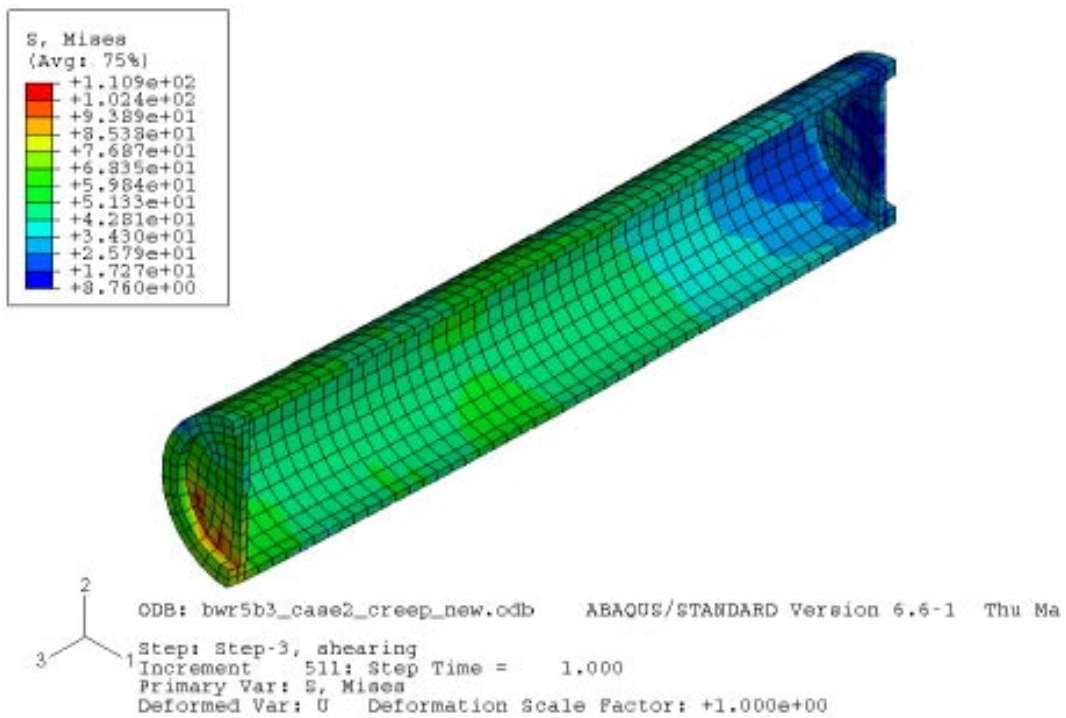


Figure A2-16. bwr5b3_case2 – Mises stress in canister after shearing 10 cm.

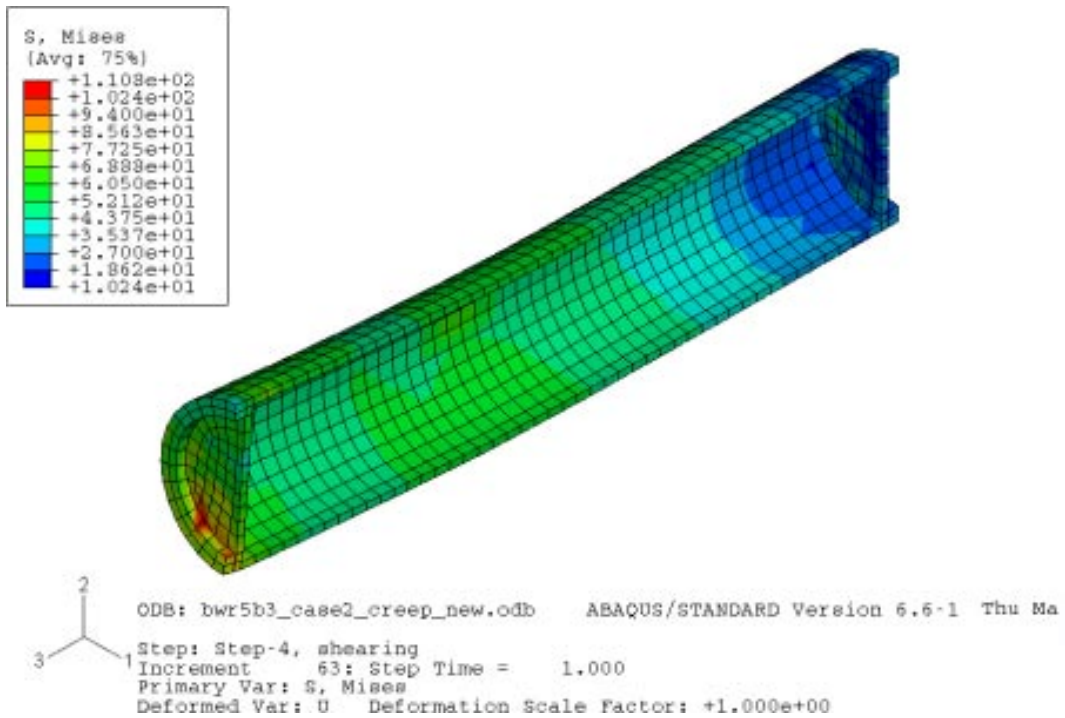


Figure A2-17. bwr5b3_case2 – Mises stress in canister after shearing 20 cm.

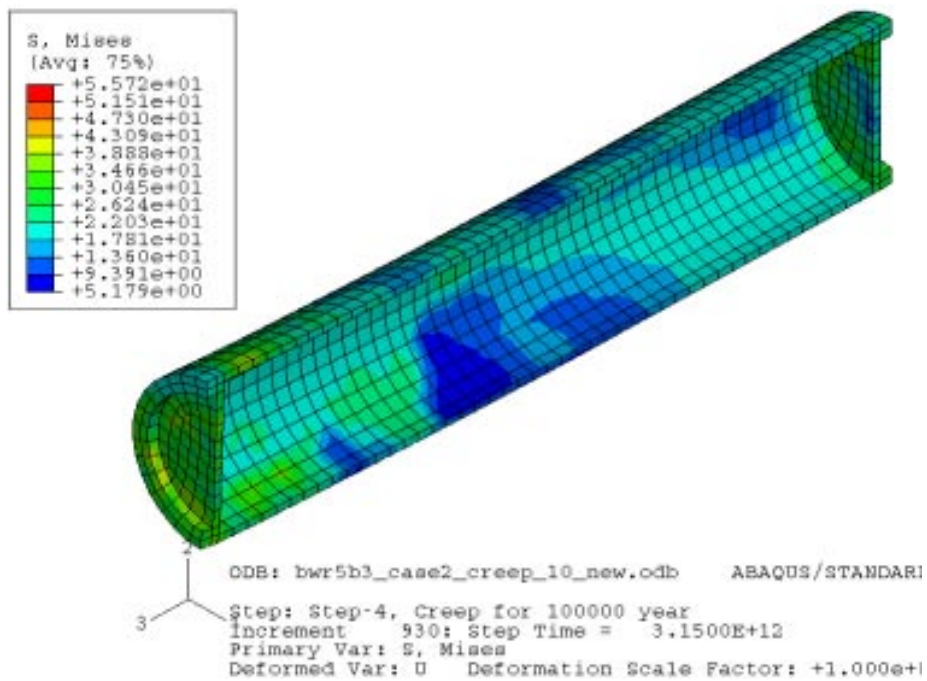


Figure A2-18. bwr5b3_case2 – Mises stress in canister after creep for 100,000 years after 10 cm of shearing.

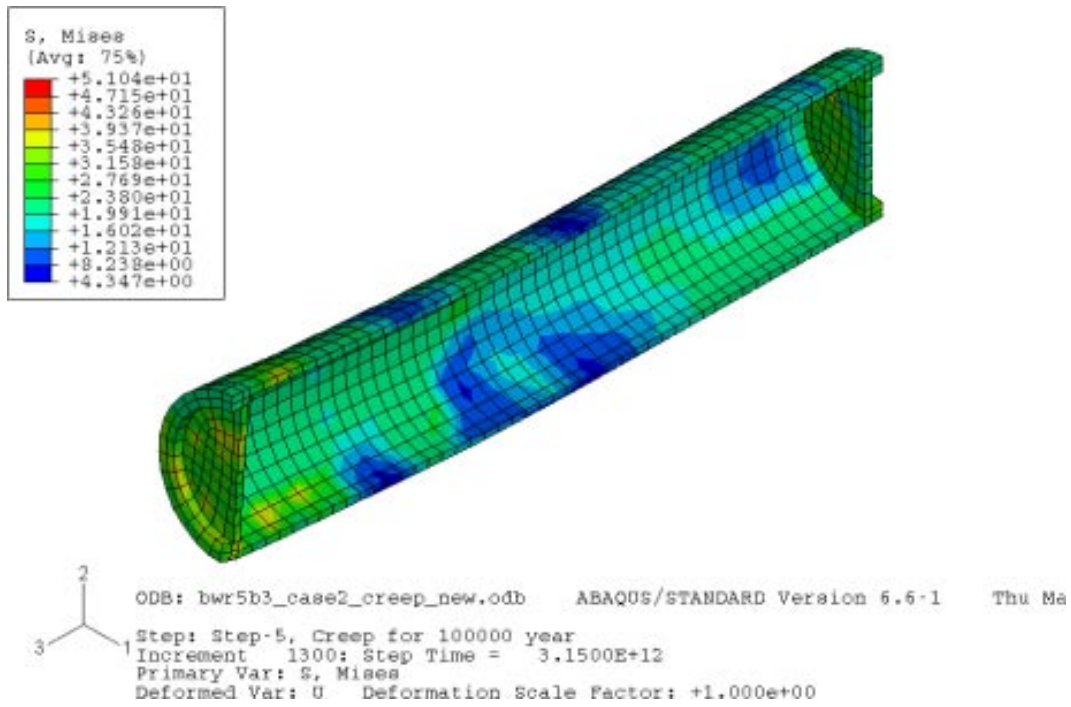


Figure A2-19. bwr5b3_case2 – Mises stress in canister after creep for 100,000 years after 20 cm of shearing.

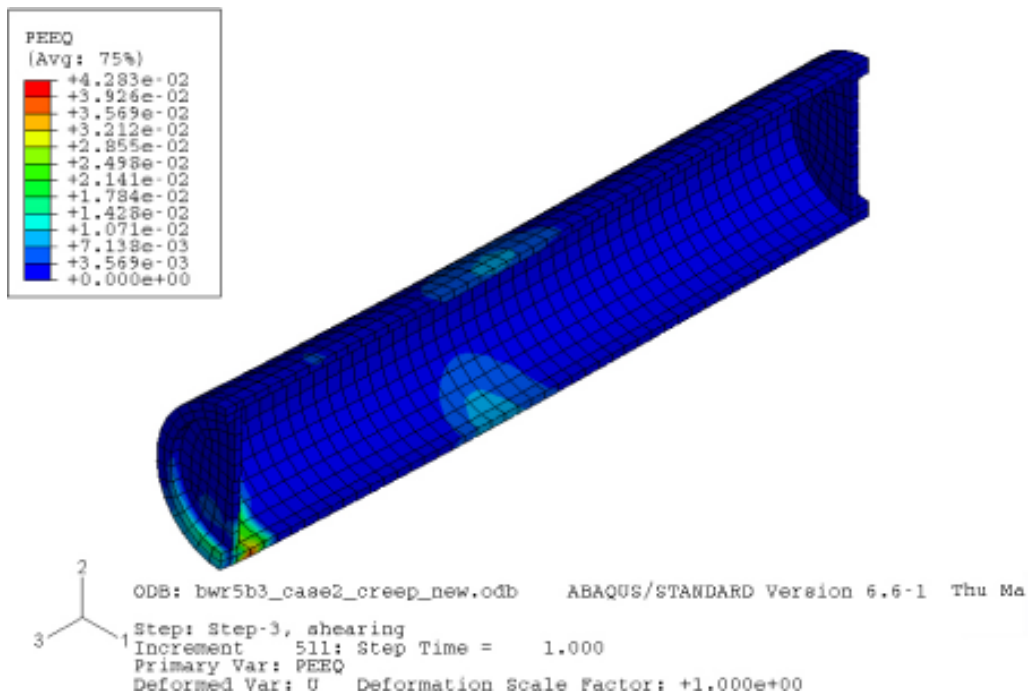


Figure A2-20. bwr5b3_case2 – plastic strain in the canister after shearing 10 cm.

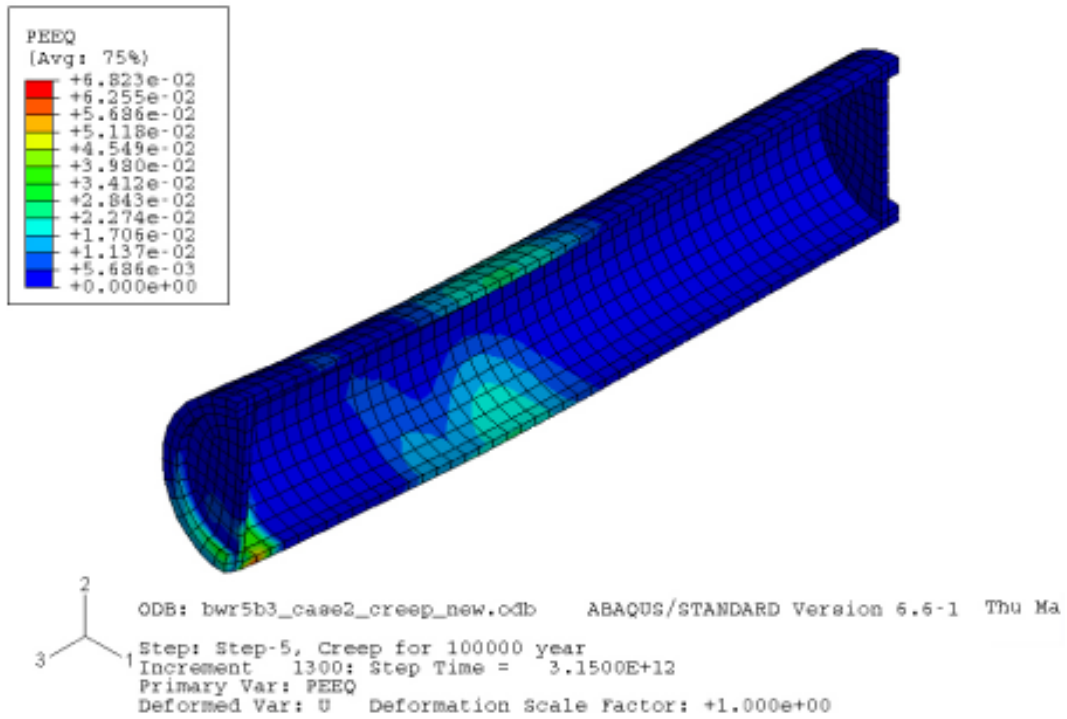


Figure A2-21. bwr5b3_case2 – plastic strain in the canister after shearing 20 cm.

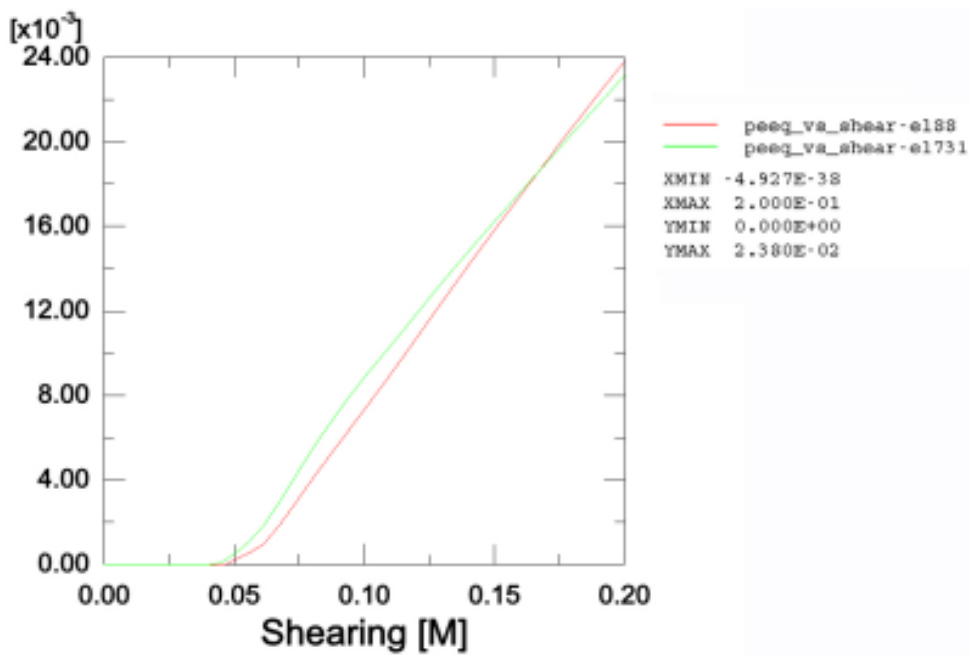


Figure A2-22. bwr5b3_case2 – maximum plastic strain in the copper after 20 cm of shearing.

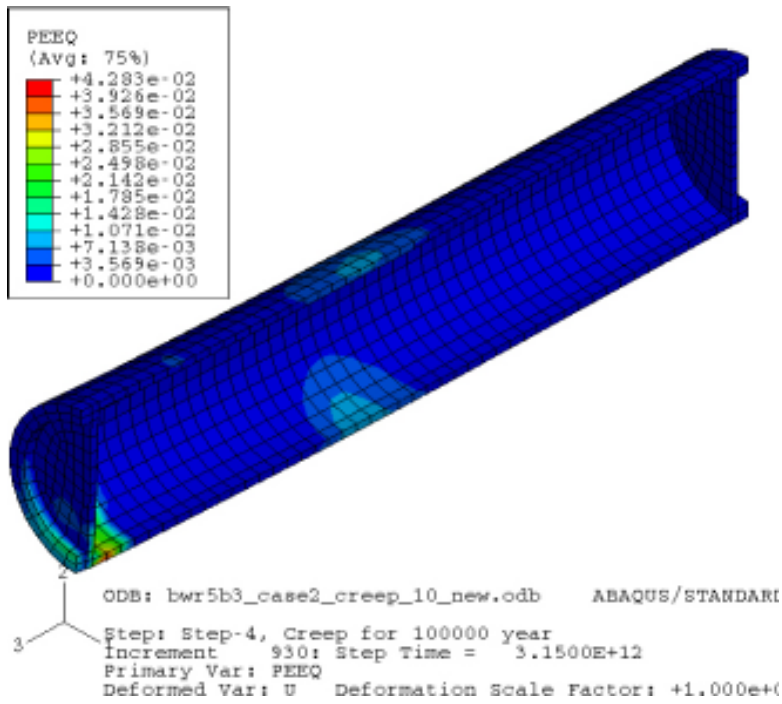


Figure A2-23. *bwr5b3_case2 – plastic strain in the canister after creep for 100,000 years after 10 cm of shearing.*

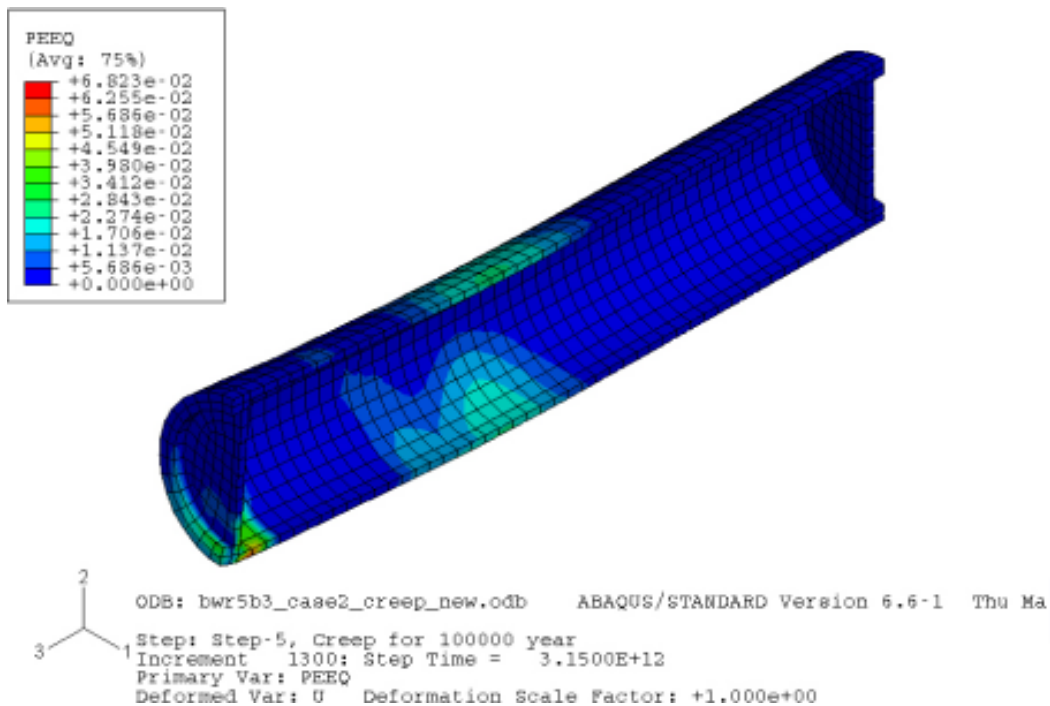


Figure A2-24. *bwr5b3_case2 – plastic strain in the canister after creep for 100,000 years after 20 cm of shearing.*

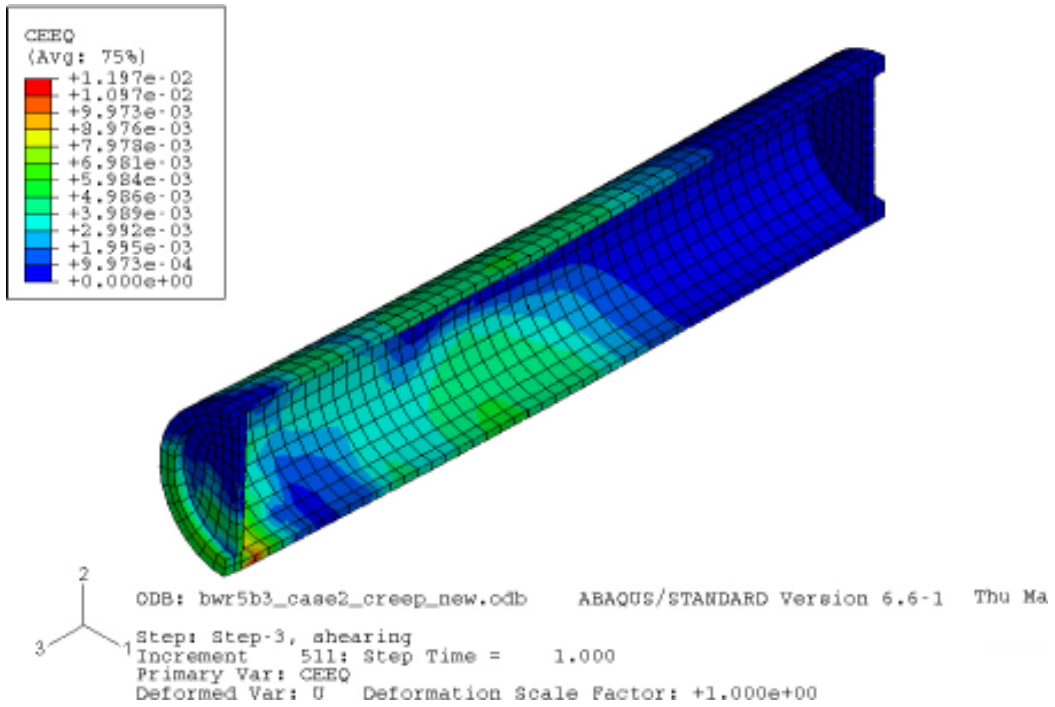


Figure A2-25. *bwr5b3_case2 – creep strain in the copper canister after shearing 10 cm.*

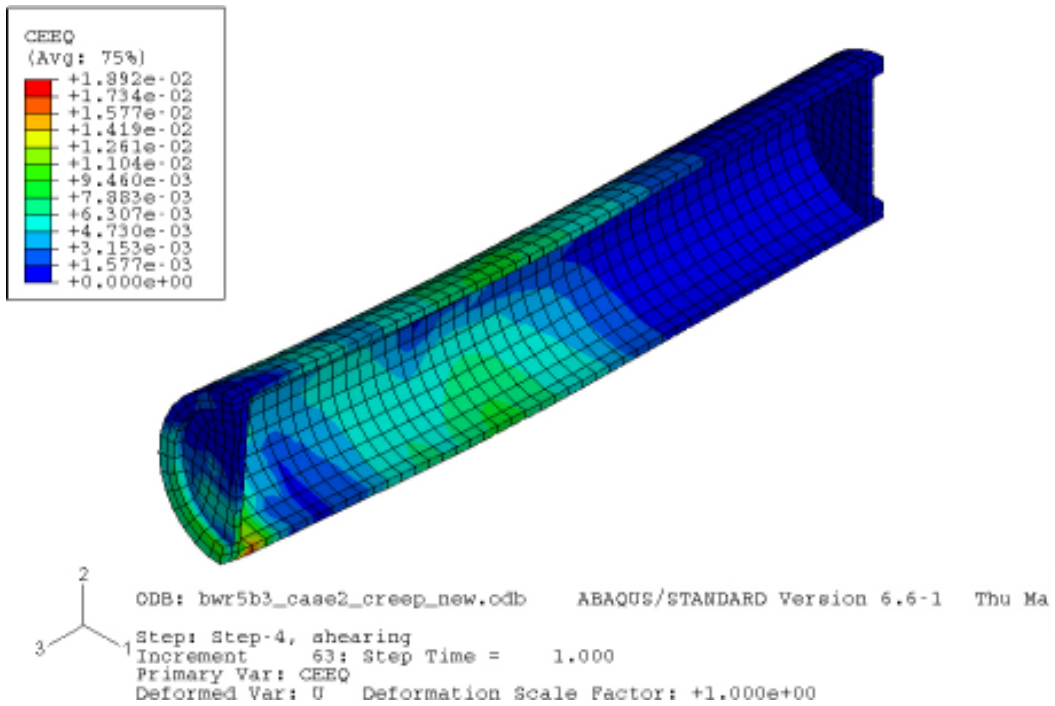


Figure A2-26. *bwr5b3_case2 – creep strain in the copper canister after shearing 20 cm.*

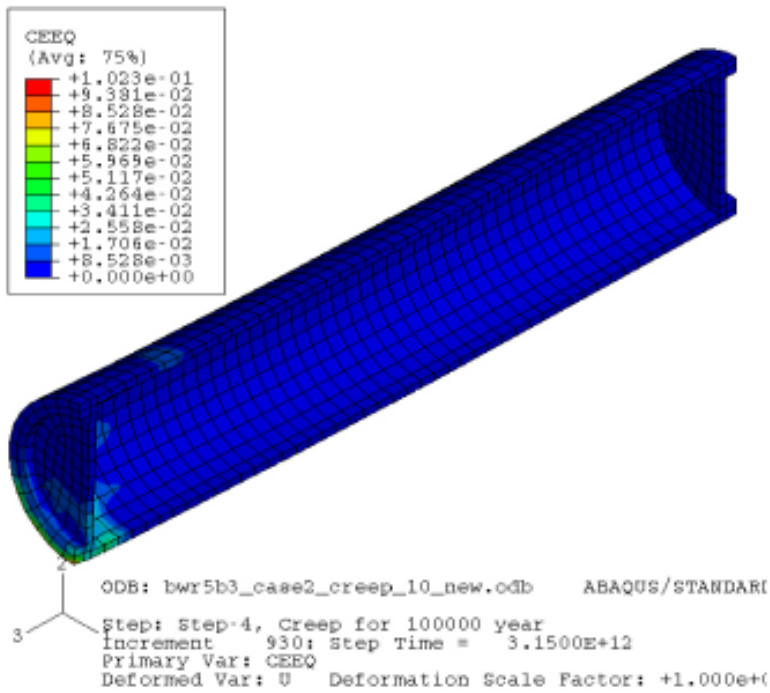


Figure A2-27. bwr5b3_case2 – creep strain in the canister after creep for 100,000 years with 10 cm of shearing.

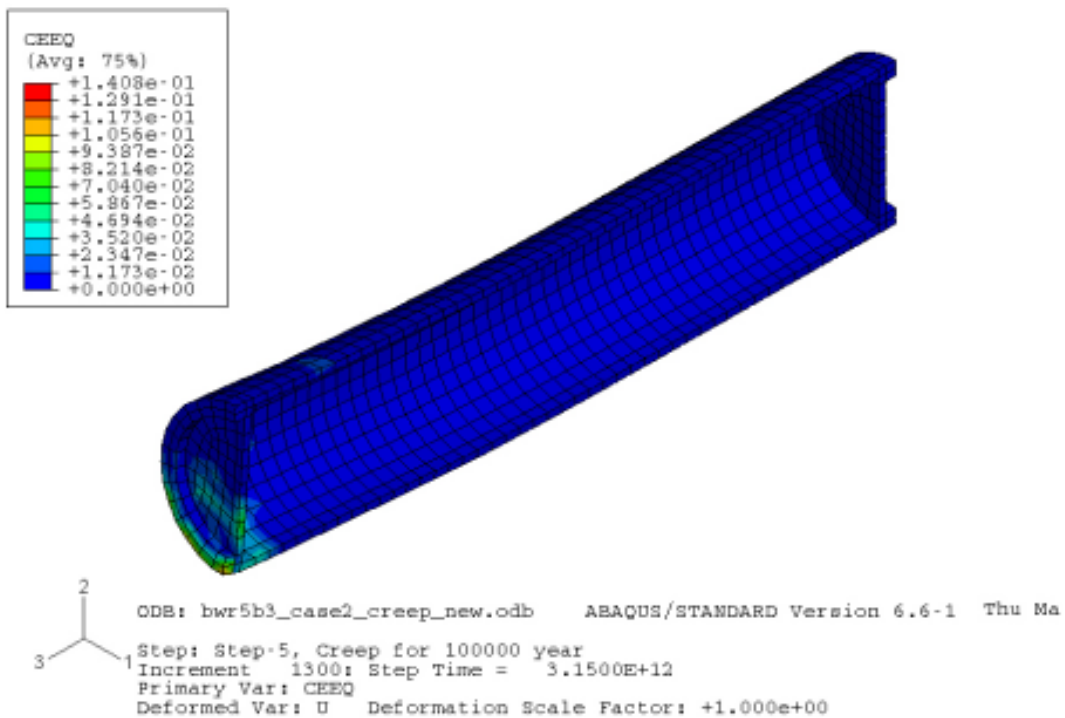


Figure A2-28. bwr5b3_case2 – creep strain in the canister after creep for 100,000 years with 20 cm of shearing.

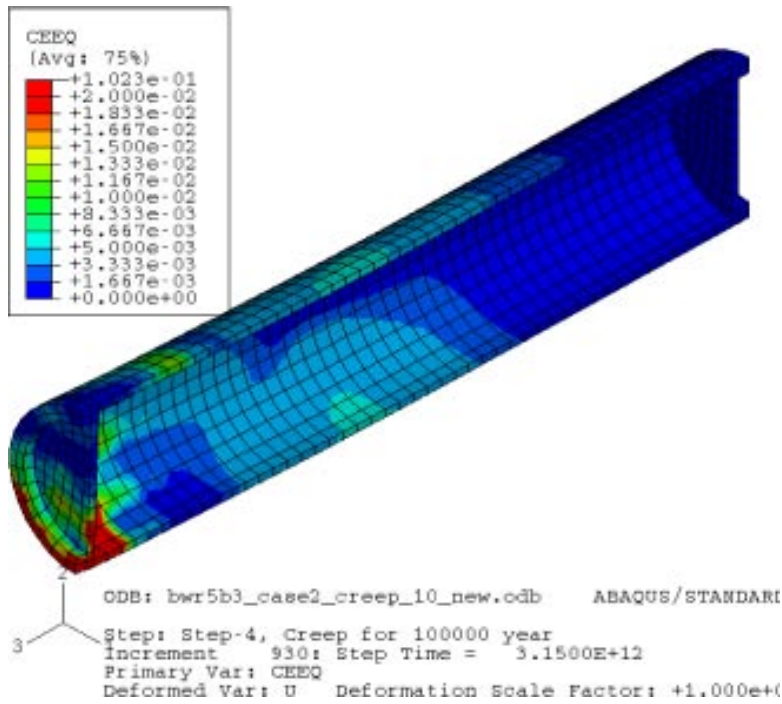


Figure A2-29. *bwr5b3_case2 – creep strain in the canister after creep for 100,000 years with 10 cm of shearing.*

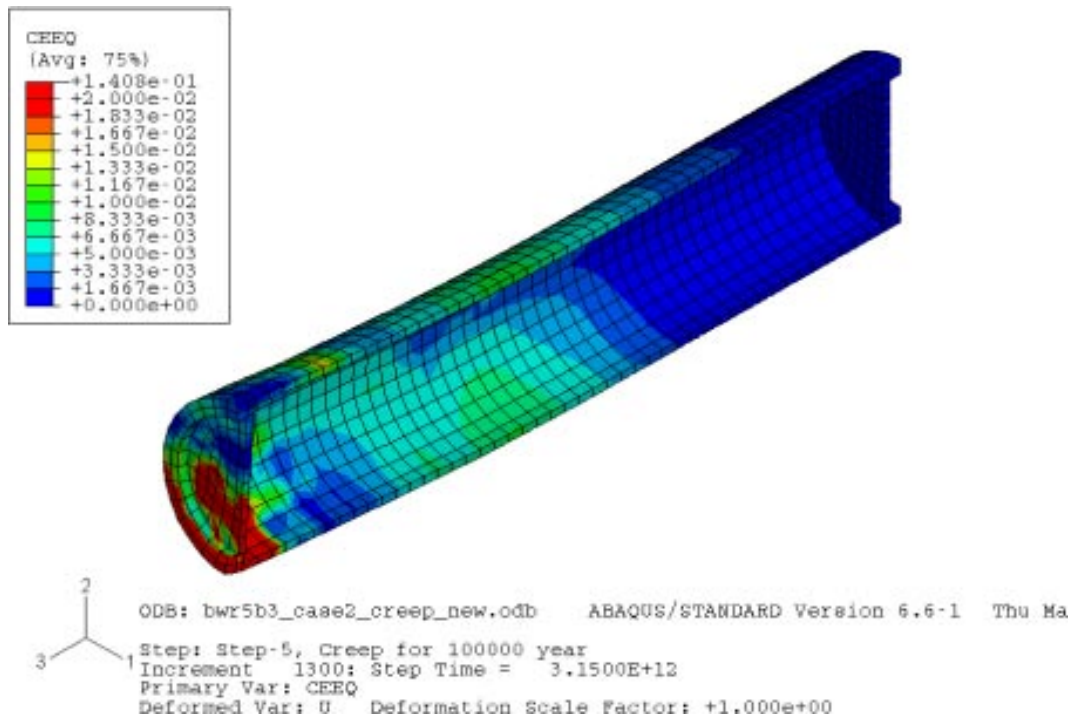


Figure A2-30. *bwr5b3_case2 – creep strain in the canister after creep for 100,000 years with 20 cm of shearing.*

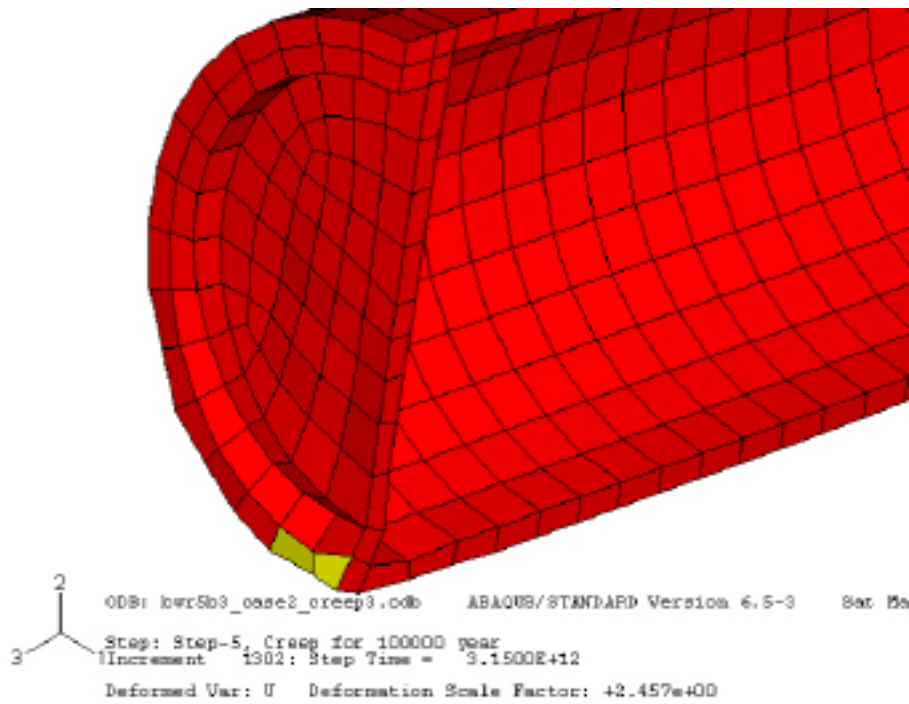


Figure A2-31. bwr5b3_case2 – element with highest creep strain after creep for 100,000 years (yellow).

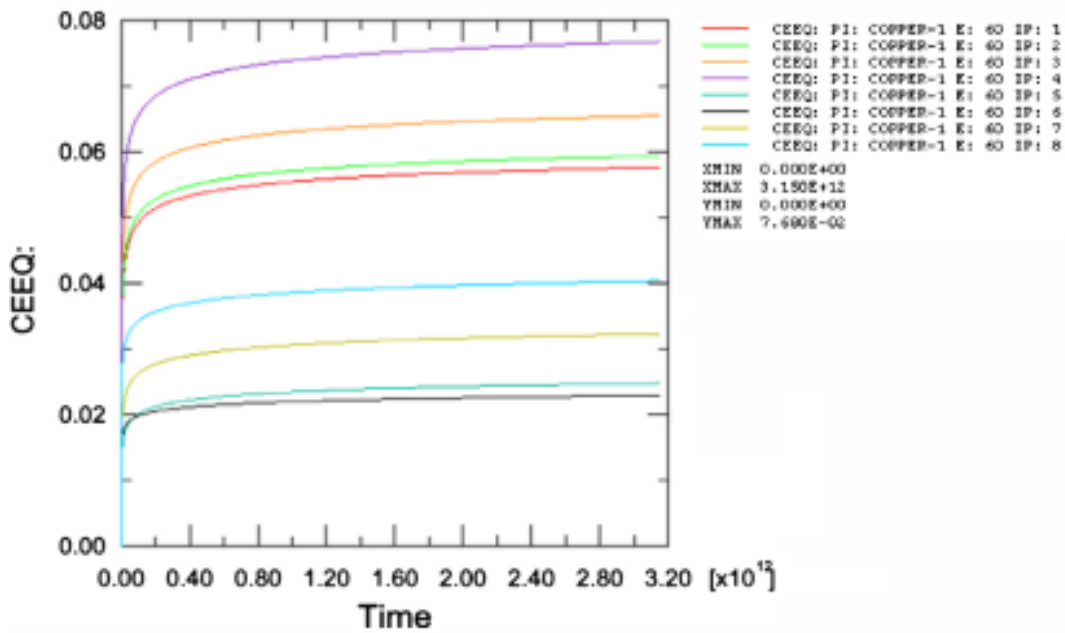


Figure A2-32. bwr5b3_case2 – creep strain in elements with highest strain of creep after shearing of 10 cm.

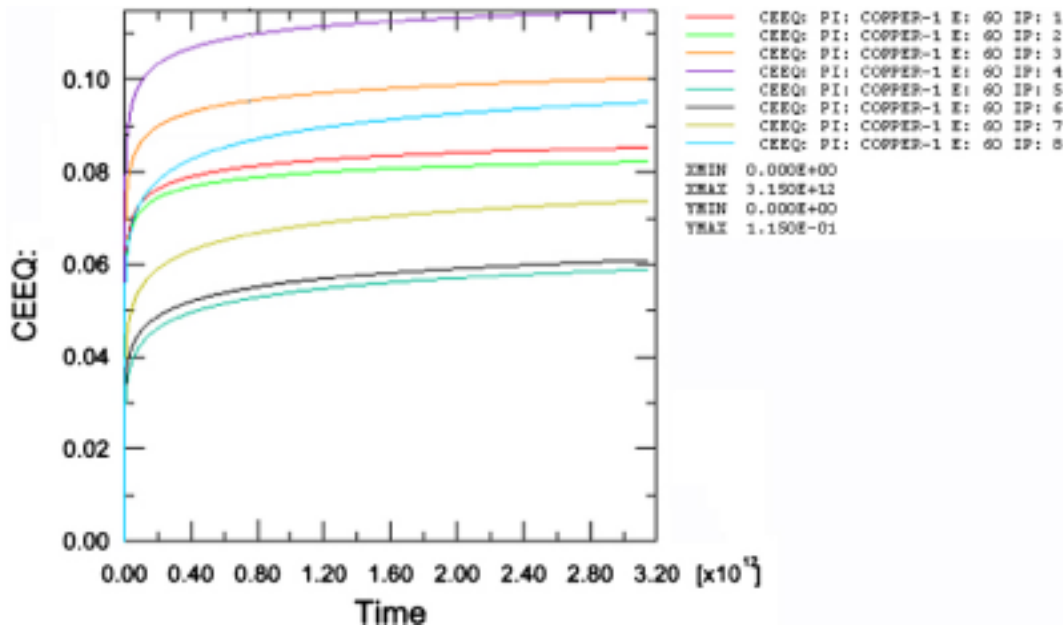


Figure A2-33. *bwr5b3_case2* – creep strain in element with highest creep strain after 20 cm of shearing.

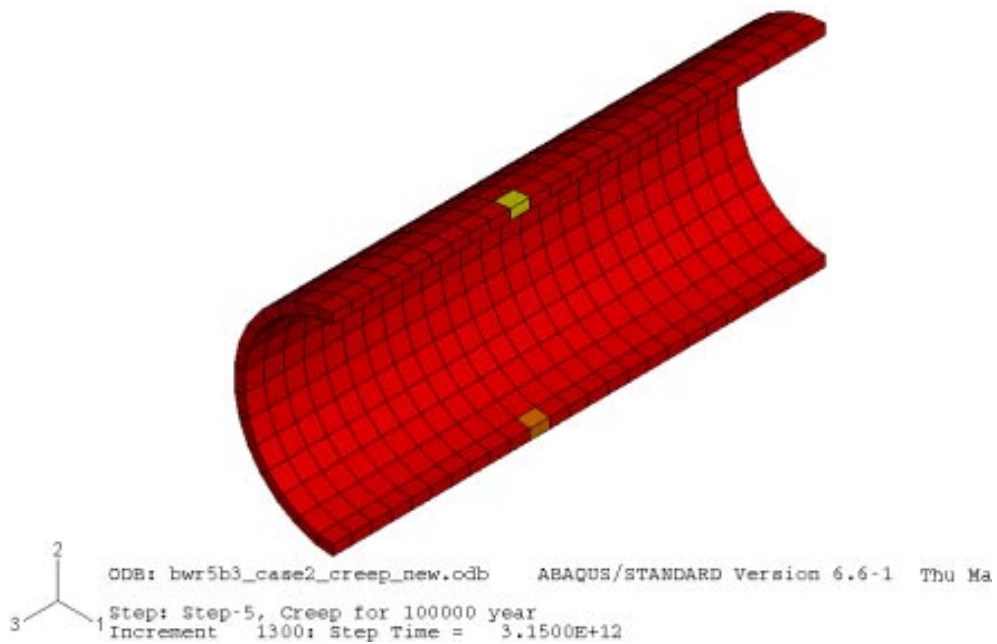


Figure A2-34. *bwr5b3_case2* – elements with maximum creep strain for the mid part of the copper cylinder.

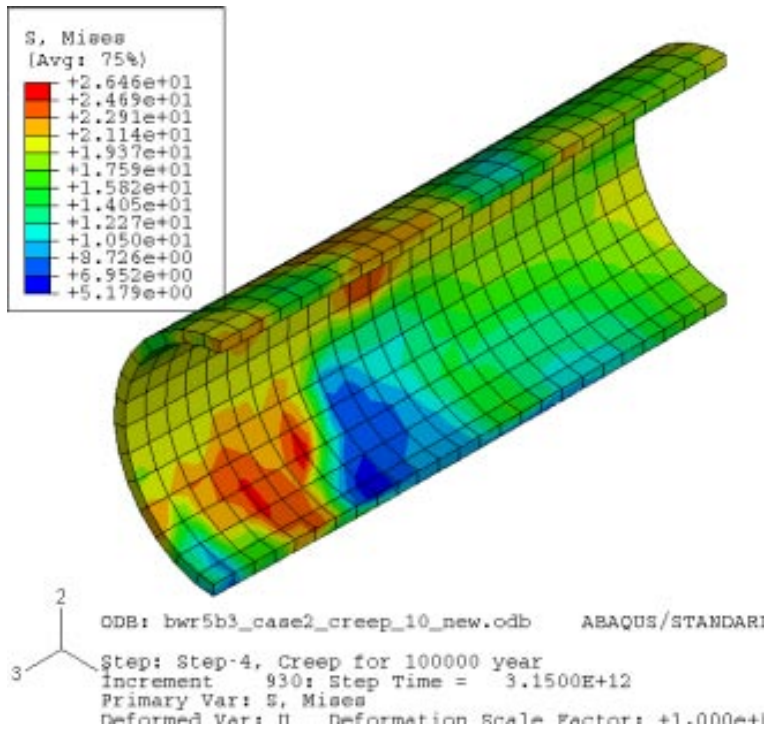


Figure A2-35. bwr5b3_case2 – Mises stress for mid part of the copper cylinder after 20 cm of shearing.

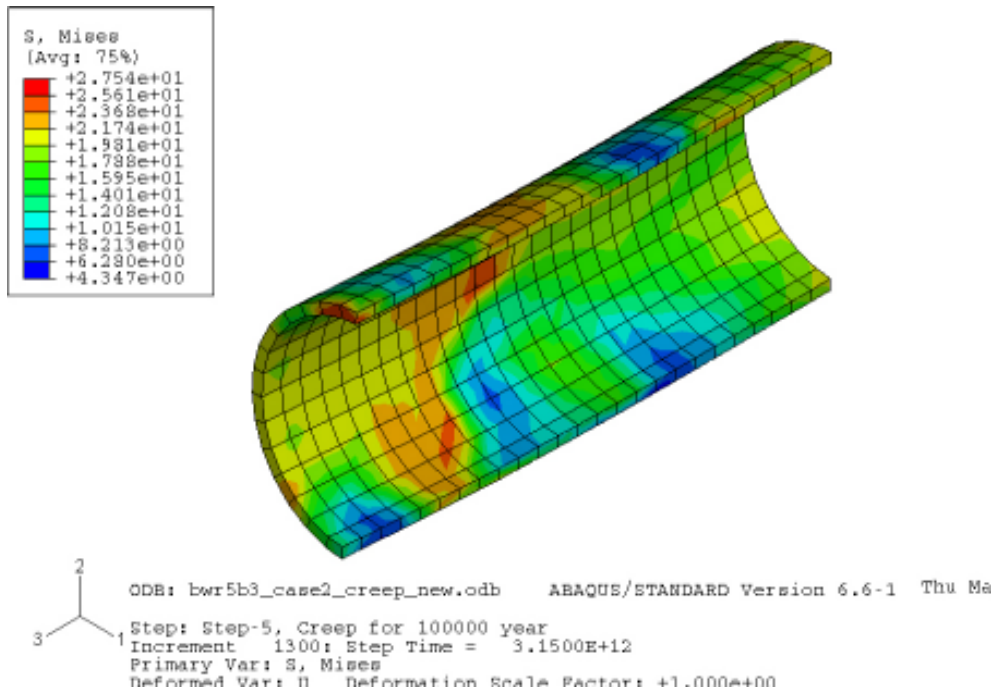


Figure A2-36. bwr5b3_case2 – Mises stress for mid part of the copper cylinder after creep for 100,000 years.

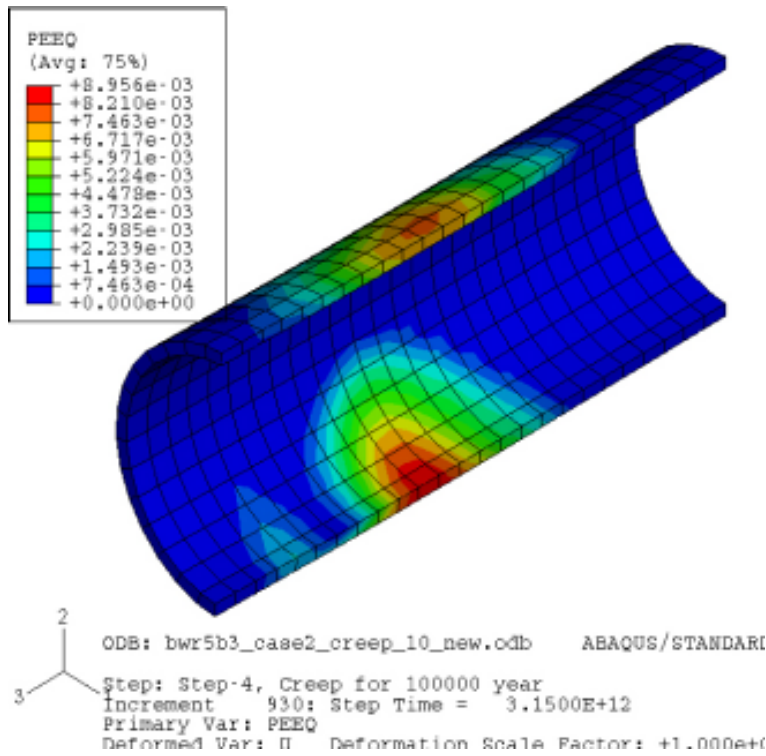


Figure A2-37. bwr5b3_case2 – plastic equivalent strain for mid part of the copper cylinder after 20 cm of shearing.

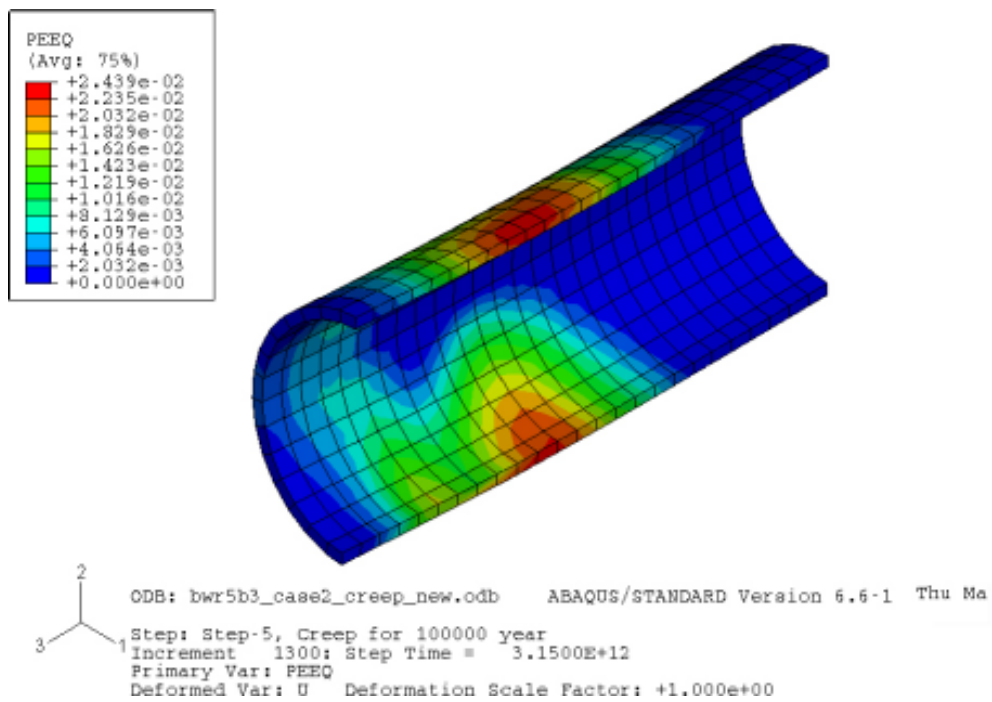


Figure A2-38. bwr5b3_case2 – plastic equivalent strain for mid part of the copper cylinder after creep for 100,000 years.

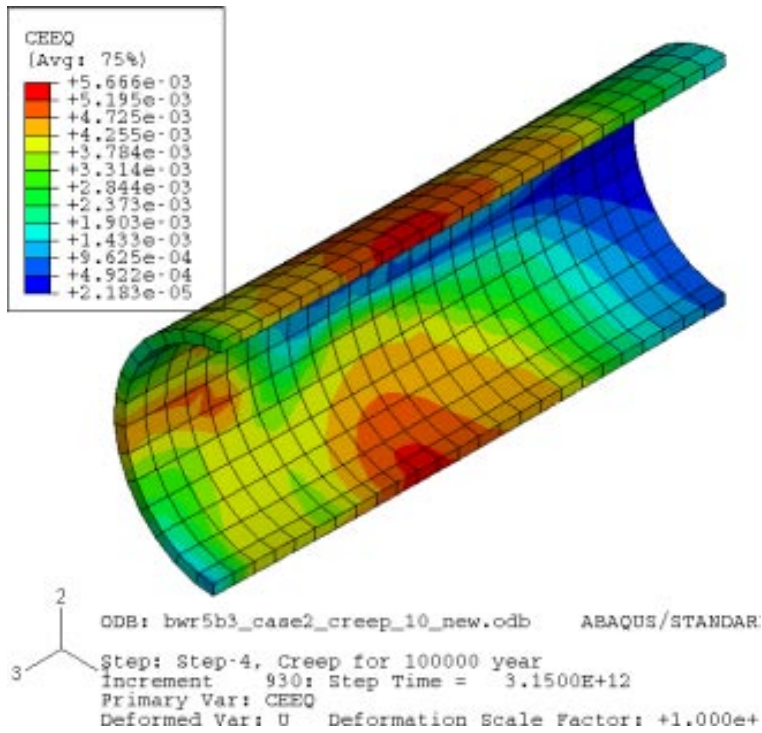


Figure A2-39. bwr5b3_case2 – creep strain for the mid part of the copper cylinder after 20 cm of shearing.

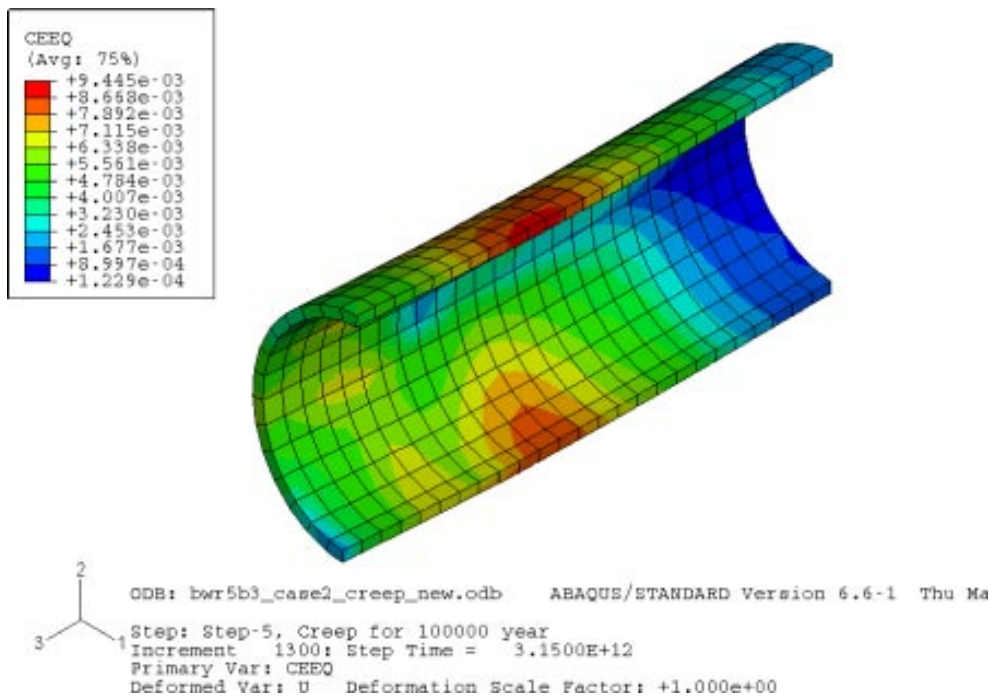


Figure A2-40. bwr5b3_case2 – creep strain for the mid part of the copper cylinder after creep for 100,000 years.

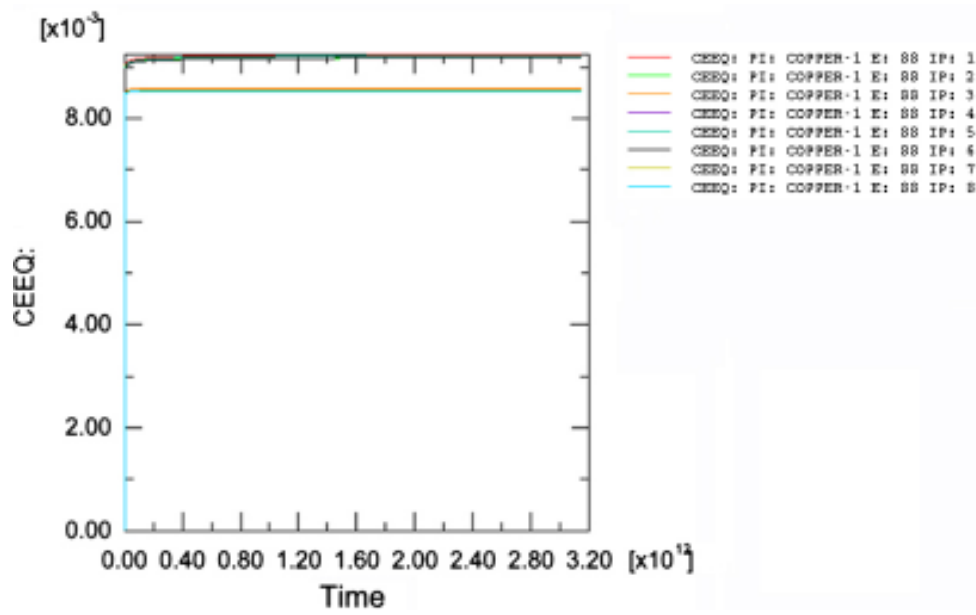


Figure A2-41. bwr5b3_case2 – element with max creep strain for mid part of the copper cylinder after 20 cm of shearing.

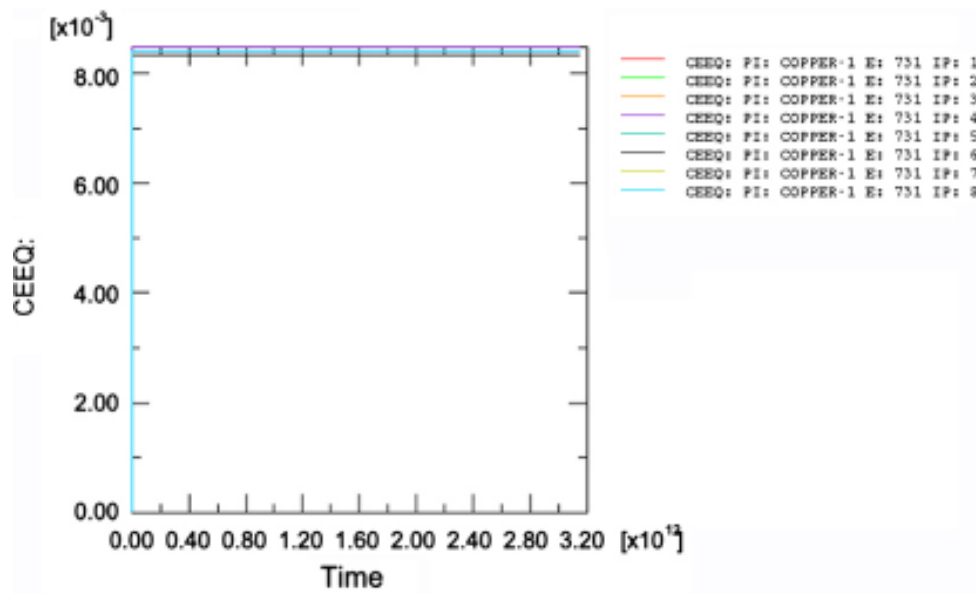


Figure A2-42. bwr5b3_case2 – element with max creep strain for mid part of the copper cylinder after creep 100,000 years.

User subroutine used for creep analysis (creep_kp)

```

C   Creep of copper
C
SUBROUTINE CREEP(DECRA,DESWA,STATEV,SERD,ECO,ESW0,P,QTILD,
1  TEMP,DTEMP,PRED,DPRED,TIME,DTIME,CMNAME,LEXIMP,LEND,
2  COORDS,NSTATV,NOEL,NPT,LAYER,KSPT,KSTEP,KINC)
INCLUDE 'ABA_PARAM.INC'
C
PARAMETER (ZERO=0.0D0,ONE=1.0D0,TWO=2.0D0,THREE=3.0D0,SIX=6.0D0)
C
CHARACTER*80 CMNAME
DIMENSION DECRA(5),DESWA(5),STATEV(*),PRED(*),DPRED(*),TIME(2),
1  COORDS(*)
C
C - Input variables
SIGMA=QTILD
T=TEMP+273
R=STATEV(1)
EP=STATEV(11)
dsig=sigma-statev(16)
hrkt_max=95.
c   if(kstep.gt.0) goto 990
   if(lflag.eq.1.or.lflag2.eq.1) then
WRITE(7,550) ' sigma0 ',kinc,SIGMA,T,R,EP,LEND,noel,npt,leximp
   end if
550 FORMAT(a,i3,4e12.3,4i6)
C
C - Constants and parameters which have been considered fixed:
C   Burgers vector [m]
B=2.5E-10
C   Taylor factor
RMS=3.06
C   Vibration frequency [1/s]
Y=1.E12
C   Shear modulus [MPa]
G=42100*(one-0.54*(T-300)/1356)
C   Mean free path parameter [m2]
RKR=2.3E-15
C   Final mean free path [m]

```

S0=4.5E-6

C Boltzmann constant [Nm/grad]
 RK=(8.31/6.023E23)*1.E-6

C

C - According to PM the best fit to tensile data was obtained with:

C Activation area [m⁴]
 A=7.0E-15

C Parameter for the shape of the curve [m²]
 OMEGA=0.25

C Parameter which determine the stress level [MPa]
 SIGMA0=20.

C Initial value of the dislocation density [m⁻²]

C R0=2.6E12 and defines under the flag *INITIAL CONDITIONS

C Initial mean free path [m]
 S1=2.8E-5

C Multiplication factor for the strain hardening
 AM=1.05

C Mobility factor
 RM=22.

C

C - functions of r

C Self diffusion coefficient, DS = f1(R,T)

C Strain rate factor, EOP = f2(R)

C Activation energy, H = f3(R,G,SIGMA)

C The mean free path for FCC, S = f4(R)

C

```

RSTART=R
dsigma=sigma-sigma0
XP=14072./T
DS=1.0E-24*R*EXP(-XP)
EOP=B*SQRT(R)*Y/RMS
H=ONE/TWO*G*B**THREE-B**TWO/SQRT(R)/RMS*(dsigma-AM*G*B*SQRT(R))
if(h.lt.zero) then
write(7,*) ' h ',h,dsigma,kinc,kstep,noel,npt
  h=zero
end if
S=S0+(S1-S0)*EXP(-RKR*R)

```

C

C - The rate equation:

```

hrkt=H/(RK*T)
if(hrkt.gt.hrkt_max) then
hrkt=hrkt_max

```



```

end if
EP=E0P*EXP(-hrkt)
DRDE=(RMS/B/S-OMEGA*R-A*R*R)
DRDT=(EP*DRDE-RM*DS*R*R)
REND=R+DRDT*DTIME
IF(LEND.EQ.0) THEN
ELSE
R=REND
DS=1.0E-24*R*EXP(-XP)
E0P=B*SQRT(R)*Y/RMS
H=ONE/TWO*G*B**THREE-B**TWO/SQRT(R)/RMS*(dsigma-AM*G*B*SQRT(R))
if(h.lt.zero) then
write(7,*) ' h ',h,dsigma,kinc,kstep,noel,npt
h=zero
end if
S=S0+(S1-S0)*EXP(-RKR*R)
hrkt=H/(RK*T)
if(hrkt.gt.hrkt_max) then
hrkt=hrkt_max
end if
EP=E0P*EXP(-hrkt)
DRDE=(RMS/B/S-OMEGA*R-A*R*R)
DRDT=(EP*DRDE-RM*DS*R*R)
END IF
DECRA(1)=EP*DTIME

```

C

C DECRA(1)=delta E, where E=epsilon=strain

C DECRA(5)=DDECRA(1)Dsigma,

C where H is the only sigma dependent variable in DECRA(1)

C

```

DECRA(2)=(Y-E0P*B*dsigma/RK/T/R)*DRDE*DTIME*
1 (B/TWO/RMS/SQRT(R))*EXP(-hrkt)

```

C

```

DECRA(5)=DECRA(1)*B**TWO/SQRT(R)/RMS/(RK*T)

```

C

C - Output variables

```

IF(LEND.EQ.1) THEN

```

```

R=REND

```

```

STATEV(1)=R

```

```

STATEV(2)=DRDE

```

```

STATEV(3)=RMS/B/S

```

```

STATEV(4)=OMEGA*R

```

```

STATEV(5)=A*R*R
STATEV(6)=DRDT
STATEV(7)=EP*DRDE
STATEV(8)=RM*DS*R*R
STATEV(9)=EXP(-H/(RK*T))
STATEV(10)=H
STATEV(11)=EP
STATEV(12)=DECRA(1)
STATEV(13)=DECRA(2)
STATEV(14)=DECRA(5)
STATEV(15)=E0P
statev(16)=qtild
statev(17)=hrkt
statev(18)=s
END IF

```

C

```
554 FORMAT(a,i5,6e12.3)
```

```
900 continue
```

```
  if(ep.gt.one) then
```

```
    WRITE(7,550) ' sigma3 ',kinc,SIGMA,T,R,EP,LEND,noel,npt
```

```
    write(7,550) ' decra ',kinc,decra(1),decra(2),decra(5)
```

```
  if(drde.lt.zero) then
```

```
    WRITE(7,554) ' varCxxx ',kinc,EP,e0p,hrkt,h,DRDE,dsig
```

```
  else
```

```
    WRITE(7,554) ' varC ',kinc,EP,e0p,hrkt,h,DRDE,dsig
```

```
  end if
```

```
end if
```

```
990 continue
```

```
  if(abs(decra(1)).lt.1e-15) then
```

```
    decra(1)=zero
```

```
    decra(2)=zero
```

```
    decra(5)=zero
```

```
  end if
```

```
END
```